The Astrophysical Journal, 618:281–296, 2005 January 1

CONSTRAINTS ON HETEROGENEOUS GALACTIC CHEMICAL EVOLUTION FROM METEORITIC STARDUST

Larry R. Nittler
Department of Terrestrial Magnetism, Carnegie Institution of Washington, 5241 Broad Branch Road NW, Washington, DC 20015
Received 2004 February 7; accepted 2004 September 8

ABSTRACT

Meteorites contain presolar grains that formed in stars prior to solar system formation and preserve a record of stellar and galactic evolutionary processes. We consider a stochastic model of heterogeneous mixing of supernova ejecta into a homogeneous interstellar medium (ISM), first presented by Lugaro et al. The predictions of the model for Si, Ti, and O isotopic ratios are compared with the compositions of presolar SiC, Al_2O_3, and $MgAl_2O_4$ grains. Model parameters that reproduce the range of Si isotopic ratios in SiC grains fail to reproduce the strong observed correlation between SiC Si and Ti isotopic ratios and the range of $^{18}O/^{16}O$ ratios in the oxide phases. The Si–Ti correlation in SiC implies that heterogeneous mixing of SNe ejecta can account for at most 40% of the range of grain isotopic compositions. This result further implies that the ejecta from diverse SNe are well mixed to the percent level in the ISM, consistent with recent results based on stellar and interstellar abundance measurements. However, the presolar grain data provide much more stringent limits on the range of relative element ratios (e.g., Mg/Fe) than can be derived from astronomical observations. The large scatter in metallicity observed for disk stars of a given age cannot be explained by heterogeneous mixing of stellar ejecta. The range of $^{18}O/^{16}O$ ratios measured in presolar oxide grains implies either that they formed in stars with a wider range of metallicities than the SiC progenitor stars or that their parent stars experienced moderate amounts of cool bottom processing.

Subject headings: dust, extinction — galaxies: evolution — ISM: abundances — nuclear reactions, nucleosynthesis, abundances — stars: AGB and post-AGB

Online material: color figures

1. INTRODUCTION

Models of Galactic chemical evolution (GCE) assume that the composition of the interstellar medium (ISM) varies smoothly as succeeding generations of stars live out their lives and synthesize new elements. A key prediction of GCE models is that stars should show an age-metallicity relation (AMR) where older stars have lower metallicity than younger stars. Such an AMR does seem to exist for the solar neighborhood (Edvardsson et al. 1993; Rocha-Pinto et al. 2000; Reddy et al. 2003), but observations over the last decade have revealed a surprising level of heterogeneity in the chemical composition of the Galaxy. For example, the range of iron abundances measured in dwarf stars in the solar neighborhood with about the same age as the Sun is far outside the range of observational errors. In terms of the usual logarithmic iron abundance ($[Fe/H] = \log(Fe/H) - \log(Fe/H)_\odot$), the 1 σ dispersion of [Fe/H] for stars of a given age has been estimated to be from 0.15 to 0.26 dex, with typical observational errors of order 0.05 dex.

A number of possible explanations for the large scatter in the solar neighborhood AMR have been proposed, including (1) heterogeneous mixing of supernova ejecta in the disk, due primarily to stochastic variations in the number, masses, types, and amount of ejecta from supernovae contributors to a given region (Malinie et al. 1993; Copi 1997; Oey 2000, 2003); (2) orbital diffusion of stars coupled with galactic abundance gradients (François & Matteucci 1993; Wielen et al. 1996; Sellwood & Binney 2002); (3) heterogeneous infall and mixing of low-metallicity material onto the disk, perhaps triggering bursts of star formation (Pilyugin & Edmunds 1996; Van Den Hoek & De Jong 1997); and (4) self-enrichment of star-forming regions (Malinie et al. 1993; Pilyugin & Edmunds 1996; Van Den Hoek & De Jong 1997). Most likely, all of these processes play some role in GCE.

One test of these various scenarios is the relative scatter in abundance ratios of different elements produced in different types or masses of supernovae (SNe). If the scatter in the AMR is due primarily to scenario (1), variations in [element/Fe] ratios should be of comparable size to the [Fe/H] ratio variations. For example, Copi (1997) reported a stochastic GCE model where different ISM regions experienced slightly different chemical enrichment histories. This model predicted a similar total range of $\sim$0.2 dex for both [Fe/H] and [Si/Fe] in the disk (Figs. 1 and 5 of Copi 1997). However, observations of local disk stars indicate that the "cosmic scatter" in element/Fe ratios is much smaller than the scatter in overall metallicity (element/H ratios). For example, Edvardsson et al. (1993) emphasized that, whereas the scatter in [Fe/H] ratios for their sample of F and G dwarfs ($\gtrsim$0.2 dex) was significant, the scatter they observed in [element/Fe] ratios was entirely accountable by the observational errors of $\gtrsim$0.05 dex ($\sim$11% on a linear scale near solar abundances). More recently, Reddy et al. 2003 came to the same conclusion for a wide range of elements and concluded that "the ejecta from the different [nucleosynthetic] sites were well mixed into the gas from which the stars formed." Thus, the current abundance data from long-lived dwarfs in the solar neighborhood can, at best, provide upper limits on the amount of chemical heterogeneity owing to incomplete mixing of supernova ejecta into the ISM. This point seems to have been missed by papers (e.g., Copi 1997; Van Den Hoek & De Jong 1997) claiming good agreement between the scatter in element/Fe ratios predicted by heterogeneous GCE models and that observed by Edvardsson et al. (1993).

Higher precision data on the relative abundances of different elements could clearly put tighter constraints on the relative importance of the different heterogeneous GCE mechanisms described above. For example, scenarios (1) and (4) both involve heterogeneous mixing of supernova ejecta in the ISM. Self-enrichment would only involve supernovae of Type II,

however, whereas scenario (1) would involve all types of supernovae. Thus, if a self-enrichment scenario was in force, one would expect larger scatter in elements whose production is dominated by SNe II (e.g., Mg) than elements also readily made in SNe Ia (e.g., Si). This was pointed out by Van Den Hoek & De Jong (1997), but observational errors do not allow for any firm conclusions to be drawn. In this paper, we consider a new high-precision source of information about GCE, namely presolar grains of stardust preserved in meteorites.

Presolar dust grains are pristine, 0.002–10 μm condensates from the winds of evolved stars that ended their lives before the formation of the solar system (Anders & Zinner 1993; Zinner 1998; Nittler 2003; Clayton & Nittler 2004). The grains were part of the interstellar medium from which the Sun formed and have survived to the present time as trace constituents of primitive meteorites (those that have not been appreciably heated on asteroid parent bodies). They are extracted from meteorites by chemical dissolution techniques and recognized as stardust by very unusual isotopic ratios in essentially every element that they contain. The observed isotopic variations are much too large to be explained by chemical or physical fractionations; instead they point to nuclear processes in stars. Although many of the isotopic signatures observed in the grains clearly reflect nucleosynthetic processes occurring in the individual donor stars themselves, some of the signatures are believed to reflect the initial compositions of the parent stars. These most likely are determined by GCE processes, and the grains can be considered an analog to the astronomical data sets used to infer the chemical history of the Galaxy (e.g., Edvardsson et al. 1993; Rocha-Pinto et al. 2000; Reddy et al. 2003). However, it is isotopic abundance ratios, rather than elemental abundance ratios, that are considered in the case of presolar grains.

This paper follows up on the work of Lugaro et al. (1999, hereafter L99), who first systematically investigated the effects of heterogeneous GCE on the silicon isotopic compositions of presolar silicon carbide (SiC) grains. As discussed in the next section, most prior work (Alexander 1993; Timmes & Clayton 1996) had primarily considered homogeneous GCE models in discussing the presolar grain data. L99 showed that a combination of homogeneous and heterogeneous GCE could easily explain the range and correlation of Si isotopic ratios measured in the SiC grains. However, their paper did not discuss other presolar stardust isotopic compositions thought to reflect GCE, including $^{18}O/^{16}O$ ratios in presolar oxide grains, and titanium isotopes in both presolar SiC and oxides. (These subjects were subsequently briefly considered by Lugaro et al. 2001, 2003). In this work, we apply the heterogeneous GCE model of L99 to these isotope systems. Our major goals are to see (1) whether the specific L99 model can simultaneously explain the isotopic data of both SiC and oxide grains, thought to have originated in similar types of stars; (2) whether multiple isotope systems can constrain the relative balance of heterogeneous versus homogeneous GCE in the ISM material from which the presolar grain parent stars formed; and (3) whether broader conclusions about GCE can be drawn from the data. A preliminary report of this work was given by Nittler (2002).

2. PRESOLAR GRAINS AND GCE

We consider here two types of micron-sized presolar stardust: SiC and refractory oxides (primarily corundum, Al_2O_3 and spinel, $MgAl_2O_4$). Both types show clustering in isotopic ratio diagrams indicating contributions from distinct stellar processes and/or source types (e.g., red giants, novae, and supernovae). This paper will focus on the dominant populations of both grain types, denoted "mainstream" for the SiC (Hoppe & Ott 1997) and Group 1+3 for the oxides (Nittler et al. 1997). Both mainstream SiC and Group 1+3 oxide grains are believed to have formed in stellar winds from low- and intermediate-mass red giant branch (RGB) and asymptotic giant branch (AGB) stars. The evidence for such an origin, based on comparisons of grain data with both astronomical observations and astrophysical models, is now very strong. The detailed arguments will not be repeated here but can be found in the literature (e.g., Anders & Zinner 1993; Hoppe & Ott 1997; Nittler et al. 1997; Zinner 1998; L99). Note that the SiC must all have originated in AGB stars, owing to the requirement that C/O be greater than unity for SiC formation. The oxides on the other hand likely originated in both RGB and O-rich AGB stars.

Si isotopic ratios measured in mainstream SiC grains are shown in Figure 1*a*. The data are presented as permil (10^{-3}) deviations from the solar (=terrestrial) isotopic ratios. The grains form a linear array of slope 1.3 on this plot, with isotopic ratios ranging from $\sim$0.95 to 1.2 times solar. The slope of the grain data is much steeper than that predicted for Si-isotopic evolution in single AGB stars ($\sim$0.3–0.8; L99). Moreover, the range of ratios is larger than that predicted for low-mass, $\sim$solar-metallicity AGB stars (<4% shifts in ratios, compared to the observed 25% range). It is evident that the mainstream Si array reflects a spread in the initial compositions of a large number of individual stellar sources (Alexander 1993; Gallino et al. 1994; Timmes & Clayton 1996; Alexander & Nittler 1999). In many presolar SiC grains, titanium is in high enough abundance to determine its isotopic composition. Ti isotopic measurements of mainstream SiC grains have indicated a similar behavior to that of Si. Namely, the $^{46,47,49,50}Ti/^{48}Ti$ ratios are correlated with the Si isotopic ratios, forming arrays on three-isotope plots with slopes distinct from those predicted for the evolution of individual AGB stars (Hoppe et al. 1994; Gallino et al. 1994; Alexander & Nittler 1999; L99). This is illustrated in Figure 2*a*, showing the observed correlation between $^{29}Si/^{28}Si$ and $^{46}Ti/^{48}Ti$ (see Fig. 4 of L99 for all Ti ratios).

Isotopic ratios are expected to change during the chemical evolution of the Galaxy, owing to metallicity-dependent nucleosynthetic yields of different isotopes (Clayton 1988). For example, the supernova yield of the "primary" isotope ^{28}Si is independent of metallicity, whereas the yields of "secondary" isotopes ^{29}Si and ^{30}Si increase strongly with increasing metallicity (Woosley & Weaver 1995; Timmes & Clayton 1996). Incorporating these yields into a GCE model, Timmes & Clayton (1996, hereafter TC96) found that the $^{29}Si/^{28}Si$ and $^{30}Si/^{28}Si$ ratios should both increase smoothly with metallicity, and hence time, assuming a monotonic age-metallicity relationship. These authors also pointed out that their GCE model fails to reproduce the solar Si isotopic composition: the calculated ISM $^{29}Si/^{30}Si$ ratio near solar metallicity is much lower than the solar ratio. They argued that this most likely reflects errors in the supernova models (both in nuclear reaction rates and the treatment of convection) and advocated a "renormalization" of the data. In this scheme, calculated isotopic ratios at all metallicities are uniformly rescaled so that the solar composition is reproduced at solar metallicity. The renormalized GCE trends for $^{29}Si/^{28}Si$ versus $^{30}Si/^{28}Si$ (TC96) and $^{29}Si/^{28}Si$ versus $^{46}Ti/^{48}Ti$ (Timmes et al. 1995, hereafter TWW95) are shown in Figures 1*a* and 2*a*, respectively. The calculated slope of the Si three-isotope trend is $\sim$1 on Figure 1*a*, shallower than the observed grain slope of 1.3. The slope of the Si-Ti trend in Figure 2*a* is in reasonable agreement with the grain data.

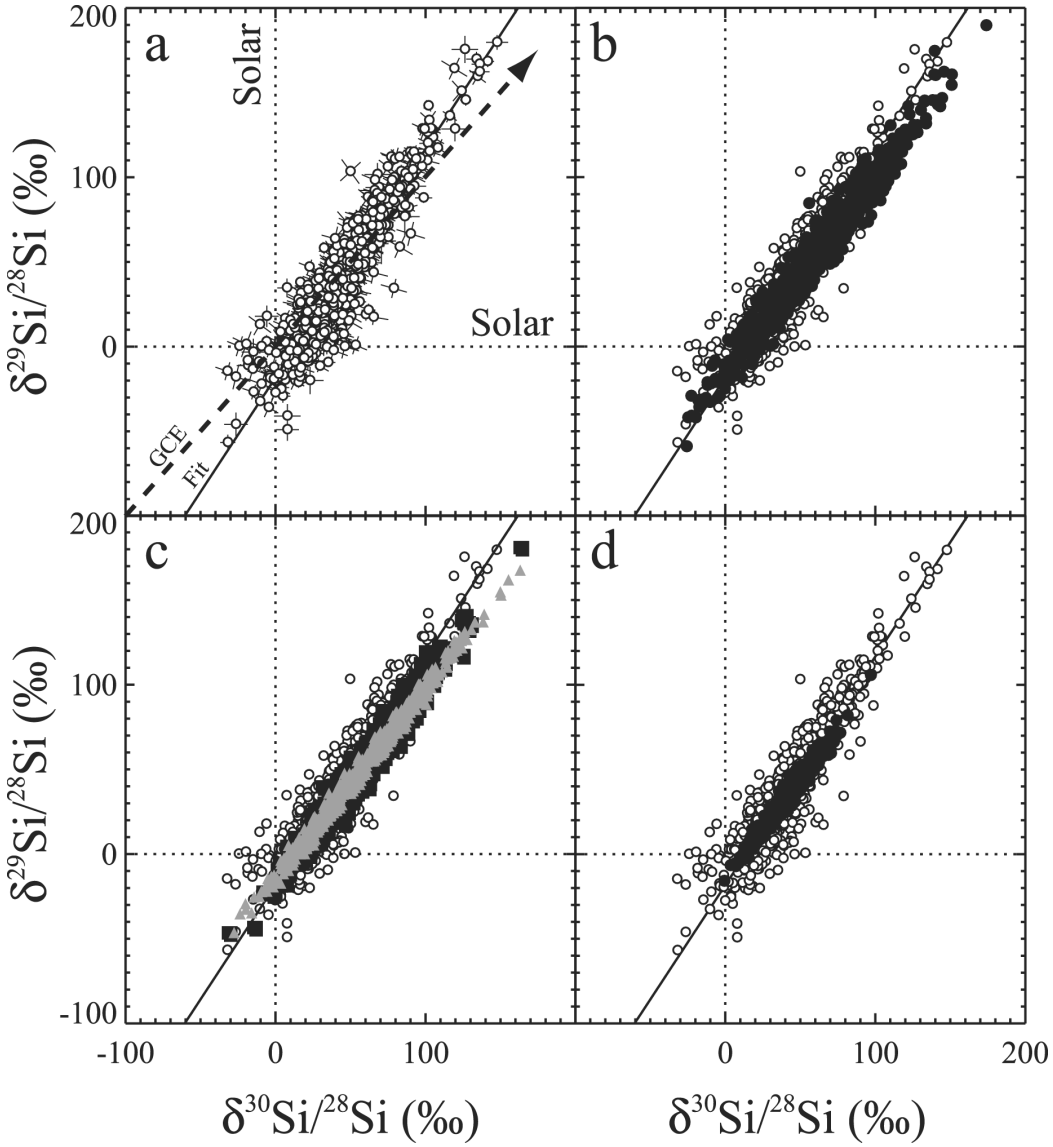

FIG. 1.—Silicon isotopic ratios of 688 "mainstream" presolar SiC grains from meteorites are compared with predictions of Monte Carlo heterogeneous GCE model. Ratios are expressed as δ values: $\delta^i\mathrm{Si} = \left[(^i\mathrm{Si}/^{28}\mathrm{Si})/(^i\mathrm{Si}/^{28}\mathrm{Si})_\odot - 1\right] \cdot 1000$. Data are from Alexander (1993), Hoppe et al. (1994), Huss et al. (1997), and Nittler & Alexander (2003). (*a*) Grain data with error bars. Dashed lines indicate calculated GCE Si isotope trend (Timmes & Clayton 1996), normalized to pass through solar. Solid line indicates the best-fit line to the data. (*b*) Standard Monte Carlo model results (*filled circles*) with parameters $a = 1.7 \times 10^{-5}$ and $N_{\mathrm{SN}} = 70$ and WW95 "B" yields for massive SNe II. (*c*) Monte Carlo model predictions for same a and N_{SN} and "A" WW95 SNe II yields (*squares*) and "C" yields (*triangles*). (*d*) Monte Carlo results (*filled circles*) for "B" WW95 SNe II yields, $a = 5.5 \times 10^{-6}$ and $N_{\mathrm{SN}} = 70$. This model represents the maximum variation allowed for the Monte Carlo model by the correlation between ^{29}Si and δ^{46}Ti in SiC grains (Fig. 2). [*See the electronic edition of the Journal for a color version of this figure.*]

The comparison of theory with the SiC grain data in Figures 1*a* and 2*a* indicate that GCE is a plausible explanation for the Si and Ti isotopic ratios in presolar mainstream SiC grains, but some important puzzles exist. First, the steeper slope of the Si isotope trend for the grains, relative to GCE calculations, cannot easily be explained. Clayton & Timmes (1997) showed that a slope 1 GCE line would be rotated into a 1.3 line on the Si δ plot, if the Sun is in fact strongly enriched in ^{30}Si, relative to the typical ISM. However, this would require that the parent stars of the mainstream SiC grains experienced far more extensive dredge-up of He-shell material than is allowed either by AGB star calculations (L99) or by the grains' ^{12}C/^{13}C ratios (Alexander & Nittler 1999). Alexander & Nittler (1999) argued, based on a fit to the SiC Si and Ti data, that the true GCE Si isotope trend has a slope closer to 1.5 than to the 1.0 value calculated by TC96. This could be the case if there were a significant nucleosynthetic source of ^{30}Si at low metallicity, not included in the GCE model of TC96. Recent calculations of ONe novae (José & Hernanz 1998) and low-metallicity AGB stars (Amari et al. 2001) suggest these as possible sources of ^{30}Si in the early Galaxy. Second, most of the SiC grains have ^{29}Si/^{28}Si and ^{30}Si/^{28}Si ratios higher than the Sun, indicating they originated in stars of higher than solar metallicity, despite having formed significantly earlier in time than the Sun. This clearly contradicts the simplest picture of homogeneous GCE. Clayton (1997) suggested that the SiC parent AGB stars formed in the inner galaxy, where more intensive star formation had led to higher metallicity and were subsequently gravitationally scattered outward to the formation radius of the Sun. However, a semianalytical study by Nittler & Alexander (1999) concluded that this process would not result in the observed SiC Si isotope distribution. Alternatively, Alexander & Nittler (1999) suggested that the Sun is slightly (~5%–10%) rich in ^{28}Si, relative to typical stars of its age and metallicity.

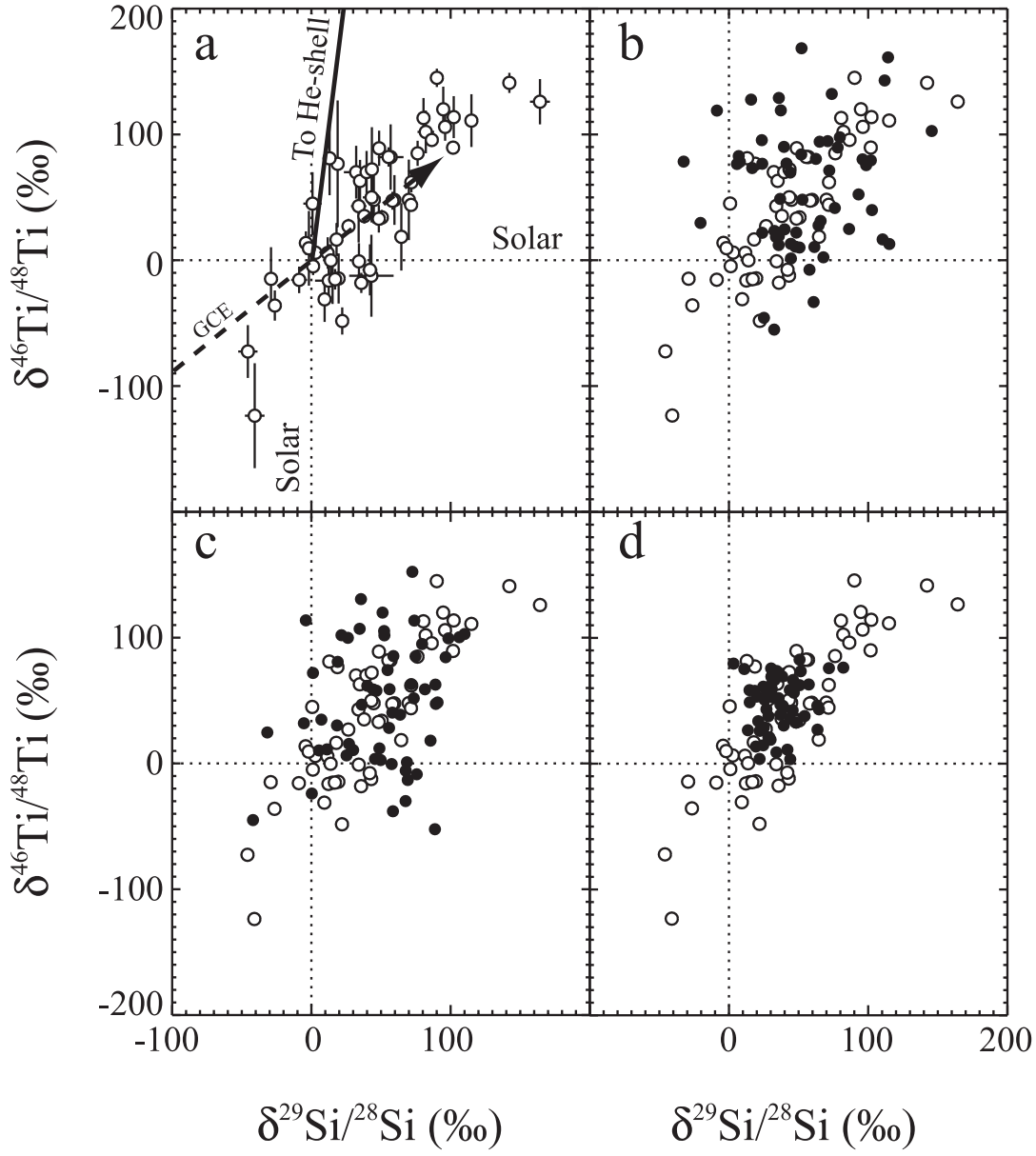

FIG. 2.—Si and Ti isotopic ratios, expressed as δ-values (see Fig. 1), of 57 mainstream presolar SiC grains compared with predictions of Monte Carlo model. Data are from Hoppe et al. (1994), Ireland et al. (1991), and Alexander & Nittler (1999). (*a*) Grain data with error bars. Dashed line is homogeneous GCE calculation of TWW95, normalized to pass through solar. The solid line indicates the trajectory of mixing with He-shell material during the third dredge-up in AGB stars (Gallino et al. 1994). (*b*) Predictions of standard Monte Carlo model (*filled circles*) with parameters $a = 1.7 \times 10^{-5}$ and $N_{SN} = 70$ and standard WW95 SNe II ^{48}Ti yields. (*c*) Monte Carlo predictions using the same parameters, but SNe II ^{48}Ti yields scaled to the WW95 ^{28}Si yields and the solar Ti/Si ratio. (*d*) Monte Carlo results (*filled circles*) for $a = 5.5 \times 10^{-6}$ and $N_{SN} = 70$ and standard ^{48}Ti SNe II yields. [*See the electronic edition of the Journal for a color version of this figure.*]

The preceding discussion was based on the assumption that stars of a given metallicity have a unique Si-isotopic composition, as follows from homogeneous GCE theory. However, as discussed in § 1, there is much observational evidence indicating chemical heterogeneity in the ISM and the need to consider heterogeneous GCE models. TC96 showed that when SNe II Si isotope yields are "renormalized" as discussed above, inhomogeneous mixing of SNe II into a solar composition was promising for producing a slope 1.3 line on the Si isotope plot, as observed in the SiC grains. L99 followed up on this suggestion and explicitly modeled, using a Monte Carlo technique, the effect of inhomogeneous mixing of SN ejecta into localized regions of the ISM. They showed that with a range of model parameters, the model could easily explain the range and scatter of mainstream SiC Si isotope ratios. They further argued that the observed distribution of SiC Si isotopes probably reflects an interplay of homogeneous GCE gradually increasing the average ISM ^{29,30}Si/^{28}Si ratios and heterogeneous GCE leading to local variations about the mean, though the balance between heterogeneous and homogeneous GCE in shaping the mainstream distribution would depend on the range of ages of the parent stars. An attractive feature of this model is that it can naturally account for the isotopic heaviness of the grains with respect to the Sun.

Although more difficult to locate in meteorites than SiC, presolar oxide minerals provide a complementary source of information about nucleosynthesis and galactic evolution (Nittler et al. 1997; Nittler 1997; Choi et al. 1998). The O isotopic ratios of most known presolar oxide grains (mostly Al_2O_3 and $MgAl_2O_4$) are shown in Figure 3. These grains were divided into four isotopic groups by Nittler et al. (1997), but we are here concerned with only those belonging to Groups 1 and 3.

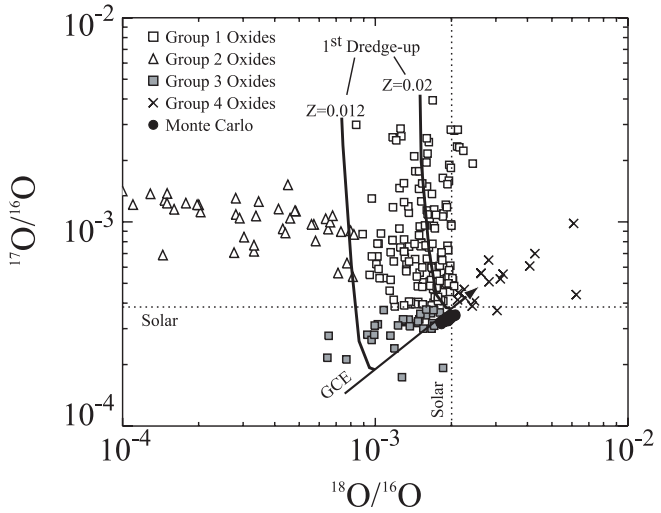

FIG. 3.—Oxygen isotopic ratios of ~250 presolar oxide grains (mostly Al_2O_3 and $MgAl_2O_4$) from meteorites, divided into groups according to Nittler et al. (1997). Data are from Nittler (1997) and references therein, Choi et al. (1998), and Zinner et al. (2003). The Group 1 and 3 grains most likely formed in O-rich red giants and AGB stars. The predicted effect of the first dredge-up on O isotopes in red giants of two different metallicities are indicated (Boothroyd & Sackmann 1999), as is the expected homogeneous GCE O isotope evolution trend (TWW95). The predictions of the standard Monte Carlo model (see Fig. 1*b* for parameters) are shown as filled circles. The Monte Carlo parameters that reproduce the range of Si isotopic ratios in presolar SiC greatly underpredict the range of $^{18}O/^{16}O$ ratios in Group 1 and 3 oxide grains. [*See the electronic edition of the Journal for a color version of this figure.*]

Together, these groups make up ~75% of the total presolar oxide population. As discussed in detail in the above cited references, the isotopic compositions of Group 1 and 3 grains most likely indicate an origin in low-mass ($M \lesssim 3\ M_\odot$) red giant and AGB stars. The large range in $^{17}O/^{16}O$ ratios observed in the grains is well-explained by convective mixing of the ashes of main-sequence partial H-burning into the stellar envelope early in the RGB phase of evolution (the "first dredge-up," see model curves on Fig. 3). However, the range of $^{18}O/^{16}O$ ratios observed in the grains is far larger than can be explained by the first dredge-up. Thus, in analogy to the Si isotopes in presolar SiC, the oxide grains' $^{18}O/^{16}O$ ratios seem to indicate a range of initial compositions of the stars (Boothroyd et al. 1994), usually attributed to GCE (see labeled curve on Fig. 3). However, if the suggestion by L99 is correct that some or all of the range of Si isotope variation in SiC might be due to inhomogeneous mixing of SN ejecta in the ISM, then an important question is how much of the range of $^{18}O/^{16}O$ ratios observed in presolar oxide grains can be explained by the same mechanism. Moreover, Ti has been measured in some presolar oxide grains as well, providing a direct method to compare SiC and oxide isotope variations.

3. MONTE CARLO MODEL

We adopt the Monte Carlo model described by L99 (see their Appendix). Basically, a small amount of the ejecta from a limited number of supernovae is admixed into a few tens to hundreds of 1 $M_\odot$ parcels of ISM material that initially had a single chemically homogeneous composition. The key parameters of the model are N_{SN}, the number of supernovae that contribute to each mix, and a, the fraction of each supernova ejecta included in the mix. The progenitor masses of Type II SNe are chosen randomly from the Salpeter (1955) initial mass function (IMF): $N(m)dM = M^{-2.35}$ dM. Note that there is considerable uncertainty in the exact form of the IMF for massive stars. For example, in a recent synthesis of various IMF estimates, Kroupa (2002) suggests that the IMF for massive stars might have a power-law slope closer to -2.70 than to the Salpeter (1955) value of -2.35. In his review of the IMF, Chabrier (2003) prefers a Salpeter value but quotes a ± 0.3 uncertainty on the slope. The IMF chosen has little effect on our results, however, as discussed further below. The number of the different types of supernovae (see below) are also chosen at random, based on a fixed average fraction of different types. This is not a GCE model in and of itself, but it approximates the effects of a single stellar generation within a stochastic GCE model (e.g., Copi 1997). Thus, it illustrates the effect of inhomogeneous mixing on the chemical compositions of stars formed at the same time in roughly the same Galactic location. It would be expected that the abundance fluctuations predicted by this model would be superimposed on the abundance trends predicted by a homogeneous GCE model.

We consider three types of supernovae: core-collapse of massive stars (Type II, Woosley & Weaver 1995, hereafter WW95), the carbon-deflagration Type Ia model W7 (Thielemann et al. 1986), and the sub-Chandrasekhar mass Type Ia model of Woosley & Weaver (1994). We assume that, on average, 80% of SNe are of Type II, 16% are the standard W7 Type Ia, and 4% are sub-Chandrasekhar mass Type Ia (hereafter subCh). These numbers differ slightly from those of L99 but are based on the numbers used by Lugaro et al. (2001) in modeling Ti isotopes (M. Lugaro 2002, private communication). An ~80:20 ratio of SNe II to SNe Ia is supported by observations (Cappellaro et al. 1999). For each calculated mixture, the numbers of W7 and subCh SNe Ia are selected from Poisson distributions with mean values of $0.16\ N_{SN}$ and $0.04\ N_{SN}$, respectively, and the number of SNe II is taken as the remaining difference between N_{SN} and the numbers of SNIa.

The ejected masses of different isotopes for SNe II are taken from the solar-metallicity calculations of WW95 (their Table 3), with some modifications described below. The mass range considered for SNe II was 10.5–42.5 $M_\odot$, because this is the range covered by the WW95 calculations. The mass of each SNe II in a given mix was randomly chosen from the IMF and the yields from the WW95 model with the closest mass used in the calculation. Yields for the W7 SN Ia model were taken from Nomoto et al. (1997) and TC96. Yields for the subCH SN Ia model were taken from Woosley & Weaver (1994). For each SN, a fraction a (in units of $M_\odot^{-1}$) is multiplied by the total ejected mass of each isotope and added to starting composition. The final mass fraction of isotope i, X^i, is then given by $X^i = X^i_{\rm initial} + \sum_i^{N_{SN}} aM^i_{\rm ejected\ SN}$. This expression assumes that the total mass of SN material added is much less than 1 $M_\odot$, a requirement always met in the cases considered here.

The ejected masses of the isotopes of O, Si, and Ti predicted by the solar-metallicity WW95 models for SNe II of masses 11–40 are shown in Figure 4. Also plotted are more recent calculations for SNe II of a limited set of masses (Rauscher et al. 2002); these models incorporated updated nuclear reaction rates and opacities compared with WW95, as well as stellar mass loss. Note that WW95 presented models of $M \geq 30\ M_\odot$ SNe II with three different assumed explosion energies, denoted "A," "B," and "C." TWW95 and TC96 used the "B" models for their GCE models, and it appears that L99 used these as well. Thus, we also concentrate on these models, but briefly discuss the effects of using the other models. For Ti, we only consider two isotopes: ^{46}Ti and ^{48}Ti. The nucleosynthesis of most Ti isotopes is poorly understood (WW95). For example, the GCE model of TWW95, using the WW95 yields, reproduces

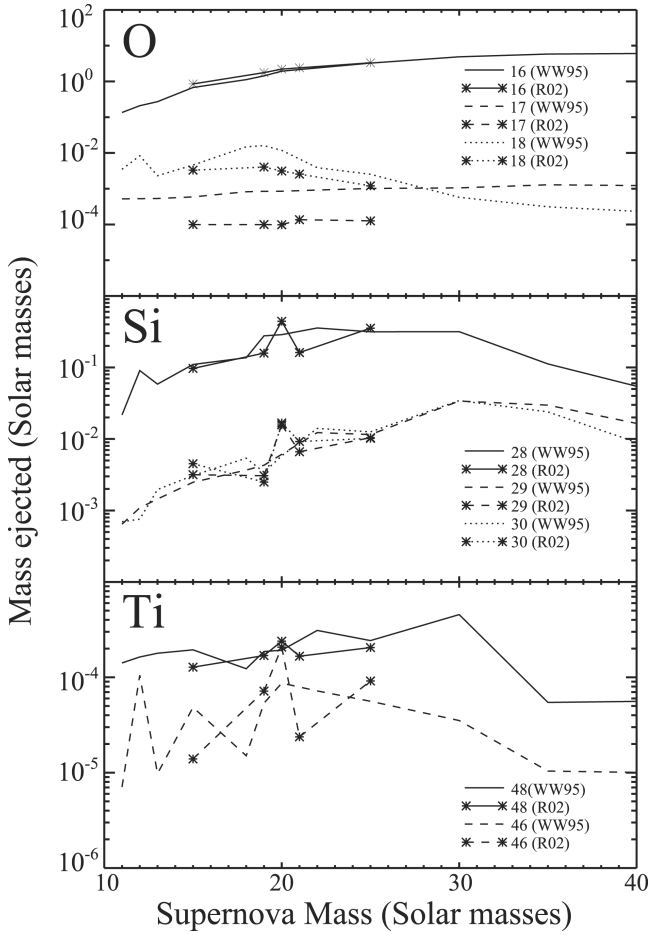

FIG. 4.—Nucleosynthetic yields from Type II supernovae as a function of progenitor mass. Recent calculations by Rauscher et al. (2002, [R02]) give similar results to those of Woosley & Weaver (1995 [WW95]) for most plotted isotopes, but obtain lower yields for ^{17}O and ^{18}O, compared to the older results.

the solar abundance of ^{46}Ti, but underproduces ^{47}Ti, ^{48}Ti, ^{49}Ti, and ^{50}Ti by factors of $\sim$6, 2, 2, and 4, respectively. Rare types of Type Ia SNe are believed to be largely responsible for the production of ^{47}Ti, ^{49}Ti, and ^{50}Ti (WW95; TWW95), but accurate model predictions are not available to include in the present calculations. Titanium observationally appears to evolve similarly to other "α" elements like ^{16}O, ^{24}Mg, and ^{28}Si (McWilliam 1997), but its calculated SNe II yields more closely match those of Fe (WW95). In our Monte Carlo calculations, we consider both the original WW95 ^{48}Ti yields and also yields based on scaling the ^{28}Si yields to the solar Ti abundance. In both cases, small additional modifications were made as discussed below.

For most of the considered isotopes, there is reasonable agreement between the recent models and the WW95 models for the SN masses that the two model sets have in common. For these, we feel confident using the WW95 yields for the Monte Carlo calculations. The only significant differences are in the yields of ^{17}O and ^{18}O, which are consistently much lower in the Rauscher et al. (2002) models, owing to updated measurements of the ^{17}O(p,α)^{14}N, ^{17}O(p,γ)^{18}F, and ^{18}O(α,γ)^{22}Ne reaction rates (Blackmon et al. 1995; Kaeppeler et al. 1994). For SNe II of masses 15–25 $M_\odot$, the recent ^{17}O and ^{18}O yields are lower than the WW95 values by factors of roughly 8 and 2, respectively. We hence multiply the WW95 yields of these isotopes by factors of 0.12 and 0.5, respectively, for the entire WW95 mass range.

In addition to correcting the O-isotopic yields for updated nuclear reaction rates, we also made small additional modifications to the yields of ^{29}Si and ^{48}Ti in the spirit of the "renormalization" procedure proposed by TC96 and discussed in the previous section. Because the current SN yields fail to reproduce the solar ^{29}Si/^{30}Si ratio, some correction must be made to directly compare theory with the grain data measured with an accuracy and precision of a few percent. The GCE calculation of TC96 overproduces all three Si isotopes at solar metallicity, but overproduces ^{28}Si and ^{30}Si by larger amounts than ^{29}Si (See Fig. 4 of TC96). Thus, the renormalization in that paper involved changes in all three isotope yields, with the smallest change to ^{29}Si. In contrast, L99 advocated increasing the ^{29}Si yield by a factor of 1.5 without modifying the ^{28}Si and ^{30}Si yields. If one is only considering Si isotope ratios, then the two schemes are equivalent, and for the "B" models of WW95 we adopt the normalization of L99 for consistency (renormalization factors for the other WW95 models are specified below). However, whether or not the ^{28}Si yield is modified could be important when considering elemental abundance ratios. For the model incorporating the original WW95 ^{48}Ti yields, we multiply all of the ^{48}Ti yields by 0.9. This ensures that the model that reproduces the Si isotopic ratios of the mainstream SiC grains also reproduces, on average, the average ^{46}Ti/^{48}Ti ratio of the grains (minus a small component due to dredge-up of He-shell material in the parent AGB stars). Similarly, for the Si-scaled ^{48}Ti yields, we apply an additional renormalization factor of 0.4. That this factor is so far below unity directly reflects the fact that the WW95 yields overproduce ^{28}Si at solar metallicity.

Note that there is an important difference between the renormalization applied here (and by L99) and that proposed by TC96. In the latter case, the calculated Si isotopic ratios for any given metallicity are scaled such that a solar-metallicity ISM has solar isotopic composition. Because these calculated ratios are essentially based on IMF-weighted averages of stellar yields, this procedure thus does not say anything about how individual stellar yields should be scaled. In contrast, in L99 and the present model, the yields of individual stars are globally scaled by the same amount regardless of their mass. This results in an IMF-weighted average matching the average grain composition (see Appendix of L99), but other scalings may well work as well and be consistent with uncertainties in nucleosynthesis calculations. We think a global renormalization has some validity for a number of reasons. First, it is the simplest approach and thus is worth investigating before trying more complicated (and arbitrary) adjustments to the yields. Second, even in the Monte Carlo model considered here, the calculated compositions are averages, weighted by an IMF, over a large number of individual SNe. Just as uncertainties in individual yields will to some extent average out in a standard GCE model, so they will in the present model. Finally, L99 showed that with this choice of scaling, the Si isotope distribution of presolar SiC grains is reproduced. Since one of our major goals is to see what additional predictions this specific model makes for other isotope systems, we must consider the same scaling originally used by those authors.

To gauge the effects of uncertainties in the SN nucleosynthesis calculations and to test how robust our conclusions are, we also calculate Monte Carlo models using an independent set of SN II yields, recently reported by Limongi & Chieffi (2003, hereafter LC03). These authors reported yields for a large number of isotopes and a grid of six SN masses (13–35 $M_\odot$). For each mass, several (6 to 12) sets of yields were given

corresponding to different characteristics of the explosions (e.g., kinetic energy). For each isotope and SNe mass considered here, we simply average the yields of the different explosion models. For the most part, the LC03 yields are similar to the WW95 yields for the O, Si, and Ti isotopes discussed here. Important exceptions are the yields of ^{29}Si, ^{30}Si, and ^{46}Ti in the most massive stars: the LC03 heavy Si isotope yields are 2–3 times lower than the WW95 ones for $M \geq 30\ M_{\odot}$ and the recent ^{46}Ti yield is $\sim$5 times higher than the WW95 one for the 35 $M_{\odot}$ model. As for the other Monte Carlo models, we must also rescale the LC03 yields in order to reproduce on average the presolar grain compositions. The renormalization factors used are 2.16 for ^{29}Si, 1.3 for ^{30}Si, and 2.0 for ^{46}Ti.

Finally, on the basis of their predicted O/Fe versus Fe/H trend, TWW95 suggested a reduction by a factor of 2 in the WW95 SNe II yields of Fe. When discussing elemental abundance ratios (§ 5.3), we will consider models both with the original WW95 Fe yields and yields reduced by a factor of 2.

4. MODEL RESULTS

Because our primary goal is to explore the predictions of the L99 model for additional isotopic systems, we do not explore the same range of parameter space that they did. Rather, we consider a limited set of parameters shown by L99 to provide a good fit to the SiC Si isotope data. Namely, most of our calculations assume $N_{\rm SN} = 70$ and $a = 1.7 \times 10^{-5}\ M_{\odot}^{-1}$ (L99, Fig. 12b). We have found that any set of parameters that provides a good fit to the Si data results in a similar range of Ti and O isotopic ratios to those reported here for these specific parameters.

Figure 1*b* shows Si isotopic ratios predicted by the Monte Carlo model compared with the mainstream SiC grain data. A total of 688 mixtures were calculated to compare with the 688 grains in the plot. For each calculated mixture of ISM material with SN ejecta, we have added a small component (δ^{29}Si = 20‰, δ^{30}Si = 25‰) to represent a typical admixture of *s*-process material from the He-shell of individual AGB stars (L99). Using the "B" SNe II yields of WW95 results in a reasonably good fit to the grain data, although the slope of the mixtures on this plot, 1.17, is in fact intermediate between the prediction of homogeneous GCE theory (1.0, TC96) and the grain data themselves (1.35). As expected, our results essentially reproduce those of L99 for the same model parameters (cf. their Fig. 12*b*). L99 did not report linear regressions to their predicted Si isotope trends, but their predicted compositions also seem to define a line of slightly shallower slope than do the grain data.

Predictions of the Monte Carlo model using the "A" (*squares*) and "C" (*triangles*) massive SNe II models of WW95 are shown in Figure 1*c*. For the calculations using the "A" models, the WW95 ^{28}Si yields were multiplied by 0.75 and the ^{29}Si yields by 1.5. The ^{29}Si yields were multiplied by 1.6 for the "C" models. These factors ensure that the calculation reproduces on average the average composition of the SiC grains. The results for these models are similar to the standard "B" case, only there is less scatter about the linear trends (i.e., higher degree of correlation between δ^{29}Si and δ^{30}Si). Moreover, the slope of the "C" trend is even lower (1.1) than the grains and the other models.

The ^{46}Ti/^{48}Ti and ^{29}Si/^{28}Si ratios predicted by the Monte Carlo model (using WW95 "B" models) are compared with the SiC grain data in Figure 2*b* for the standard WW95 ^{48}Ti yields and in Figure 2*c* for the Si-scaled ^{48}Ti yields. A total of 57 Monte Carlo mixtures are plotted to compare with a similar number of plotted grain data. A fixed value of 53‰ was added to predicted δ^{46}Ti values to reflect dredge-up in individual AGB stars (L99). Using either set of SNe II Ti isotope yields, the model predicts a similar total range of ^{46}Ti/^{48}Ti ratios to that observed in the grains. However, unlike the case for the Si three-isotope plot, the correlation between Si and Ti isotopic ratios observed in the grains is not reproduced by the Monte Carlo model. This important result is discussed in detail below. Lugaro et al. (2001) reported similar results for these isotope ratios.

The Si and Ti isotopic ratios predicted by the Monte Carlo model using the Limongi & Chieffi (2003) SNe II yields are compared with the SiC data in Figure 5. Because of differences between these yields and those of WW95 used above, obtaining a good match to the SiC data requires different values of the model parameters a and $N_{\rm SN}$. Figures 5*a* and 5*b* correspond to a case with $a = 5 \times 10^{-5}$ and $N_{\rm SN} = 40$. Clearly, this case gives similar results to the model using the WW95 yields and $a = 1.7 \times 10^{-5}$ and $N_{\rm SN} = 70$ (Figs. 1*b*, 2*b*, and 2*c*). As before, the range and correlation of Si isotopic ratios observed in presolar SiC grains can be well reproduced by the model. However, although the LC03 yields do lead to some correlation between ^{29}Si/^{28}Si and ^{46}Ti/^{48}Ti ratios (Fig. 5*b*), the predicted range and correlation of these ratios are still a poor match to the grain data, as was the case with the previous models. The similarity of the results obtained using independent calculations of SN nucleosynthesis indicates that, to first order, our results are not significantly affected by uncertainties in the yields of individual supernovae.

O isotope predictions of the Monte Carlo model (using WW95 "B" models) are compared with the Group 1+3 presolar oxide grains in Fig. 3. Two hundred mixtures were calculated to compare with a similar number of grains. The mixtures are in general enriched in ^{16}O, relative to the heavier isotopes of oxygen and the starting composition. The average shifts from the starting ratios are -12% for ^{17}O/^{16}O and -3.4% for ^{18}O/^{16}O. This is in contrast to the case of Si, where most of the mixed compositions are isotopically heavy, relative to the starting solar composition, and reflects the reduced yields of ^{17}O and ^{18}O in recent SNe II models (Rauscher et al. 2002). Calculations using the WW95 "A" and "C" models for the most massive SNe II yield similar results, but with slightly higher and lower average ratios, respectively. In all cases, the majority of mixtures are enriched in ^{16}O, relative to the starting solar composition, however. Because the O isotope SNe II yields predicted by LC03 are very similar to the scaled WW95 yields used here, using them in the Monte Carlo model gives very similar results to those shown in Figure 3, and thus we do not show them.

The O-isotopic ratios, especially ^{17}O/^{16}O, of the presolar grains have been strongly affected by the first dredge-up process in their parent stars (Boothroyd & Sackmann 1999; Nittler et al. 1997; dredge-up curves in Fig. 3) and therefore the total range of compositions would not be expected to be reproduced by the present model. One can subtract a first dredge-up component from the grains' O-isotopic ratios by projecting grain compositions along curves parallel to the dredge-up model curves of Boothroyd & Sackmann (1999) onto the assumed GCE line (Fig. 3). A histogram of initial ^{18}O/^{16}O ratios inferred for the grains in this way is compared with the Monte Carlo predictions in Fig. 6. Note that a significant fraction of the oxide grain data set was identified using an automated method searching for grains with anomalous ^{18}O/^{16}O ratios (Nittler et al. 1997). Since many Group 1 grains have ^{18}O/^{16}O ratios close to the solar value, but unusual ^{17}O/^{16}O ratios, this method introduced a bias into the data set toward grains with anomalous

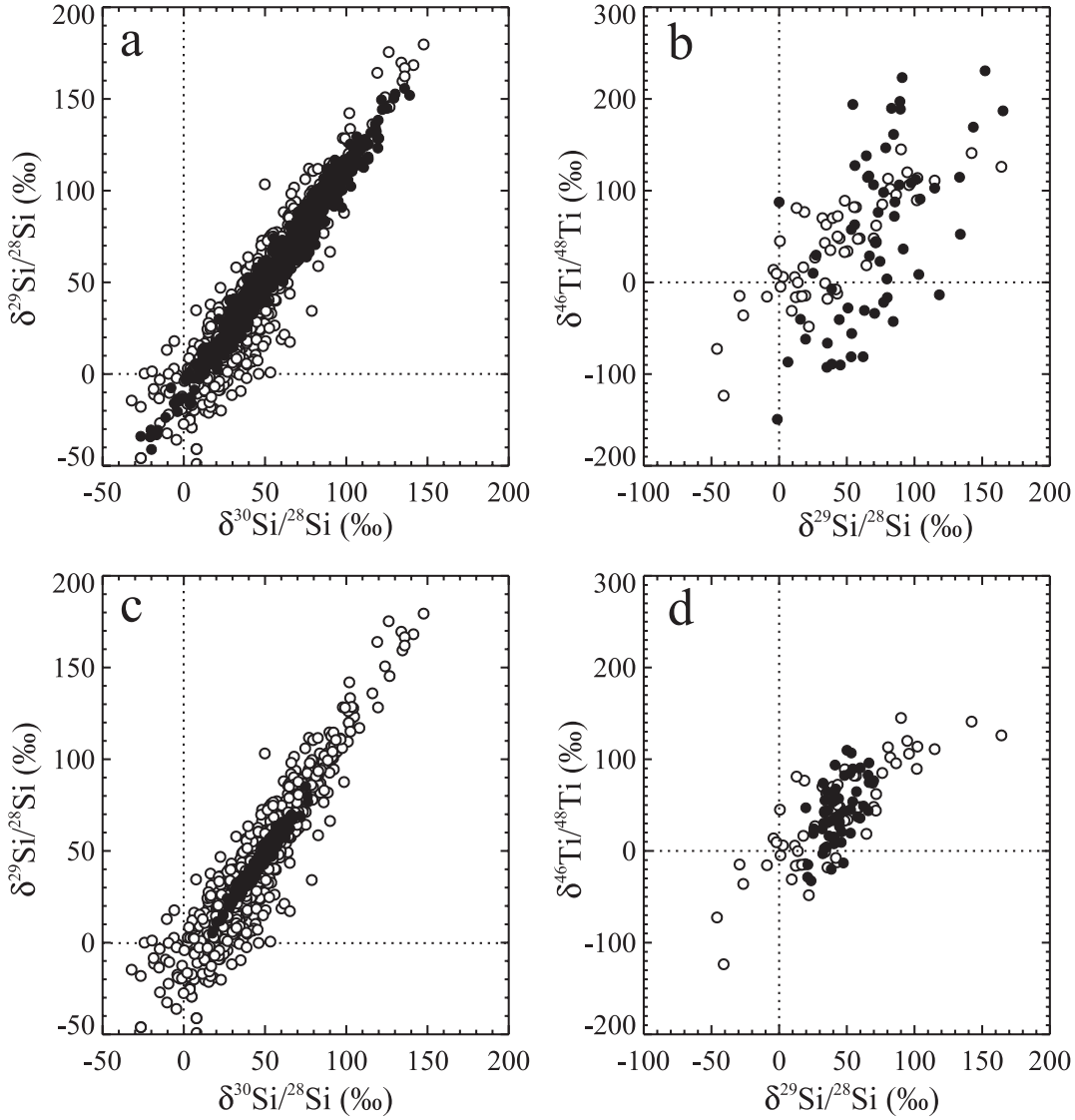

FIG. 5.—Si and Ti isotopic ratios of presolar SiC grains (*open circles*; see Figs. 1 and 2 for data sources) are compared with predictions of the Monte Carlo model using SNe II yields of Limongi & Chieffi (2003). (*a, b*) Monte Carlo results using parameters $a = 5 \times 10^{-5}$ and $N_{SN} = 40$. As for the standard Monte Carlo case (cf. Fig. 1*b*), the model can explain well the range and correlation of SiC Si isotopic ratios but fails to reproduce the strong correlation between δ^{29}Si and δ^{46}Ti values. (*c, d*) Results for model parameters $a = 1.3 \times 10^{-5}$ and $N_{SN} = 70$. This model represents the maximal variation allowed for the Monte Carlo model by the correlation between δ^{29}Si and δ^{46}Ti in SiC grains (cf. Figs. 1*d* and 2*d*). [*See the electronic edition of the Journal for a color version of this figure.*]

$^{18}O/^{16}O$ ratios. To avoid this bias in Figure 6, we have only included grains identified by measurements of all three stable O isotopes. Clearly, the Monte Carlo model parameters that reproduce the range of Si isotopes in mainstream SiC grains do not reproduce the range of initial $^{18}O/^{16}O$ ratios of the presolar oxide grain parent stars. The relative standard deviation of the initial $^{18}O/^{16}O$ ratios inferred for the Group 1 and 3 oxide grains in Figure 6 is 24%, a factor of ~8 times that of the Monte Carlo predictions (2.9%). Conversely, any heterogeneous model that would reproduce the range of $^{18}O/^{16}O$ ratios of the presolar oxide grains would predict a much larger range of Si isotope ratios than are observed in presolar SiC grains.

Low Ti abundances and small grain sizes have limited the number of Ti isotopic measurements in presolar oxide grains, but Ti data have been reported for a small number of grains (Choi et al. 1998; Hoppe et al. 2003). Figure 7 compares the predictions of the standard Monte Carlo model with the Group 1 and 3 oxide grains for which Ti isotopic data are available. Unfortunately, terrestrial contamination cannot be ruled out for those grains with Ti isotopic compositions close to solar, since Ti is a trace element in the presolar Al_2O_3 grains. The seven grains with $^{46}Ti/^{48}Ti$, $^{47}Ti/^{48}Ti$, or $^{49}Ti/^{48}Ti$ ratios more than 2.5 σ away from the terrestrial ratios are indicated by a half-filled square symbol (^{50}Ti measurements are often compromised by the presence of isobaric interference of ^{50}Cr). The dashed line indicates a linear regression to these grains, while the solid line indicates the predicted GCE trend, from the model of TWW95, normalized to pass through the solar composition. The Monte Carlo results are roughly compatible with the range of $^{46}Ti/^{48}Ti$ measured in grains with near-solar inferred initial $^{18}O/^{16}O$ ratios, but the small number and large error bars of these grains limits the usefulness of the comparison. The seven grains with Ti anomalies, especially the two grains with the most extreme compositions, indicate a positive correlation between $^{18}O/^{16}O$ and $^{46}Ti/^{48}Ti$. Such a correlation is expected from GCE models (TWW95), but not predicted by the Monte Carlo model.

As mentioned in the previous section, there is some uncertainty in the slope of the initial mass function for massive stars in the Galaxy. A range of studies (reviewed by Kroupa 2002 and Chabrier 2003) indicate an average power-law IMF slope of

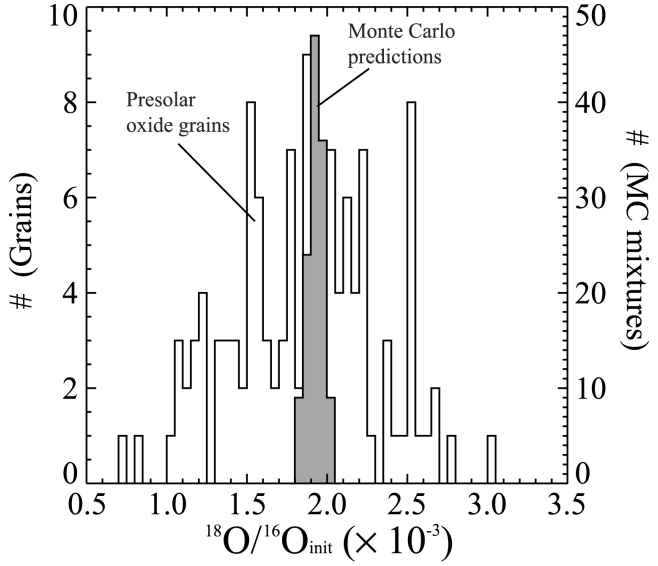

FIG. 6.—Distribution of initial $^{18}O/^{16}O$ ratios inferred for Group 1 and 3 presolar oxide grains (Fig. 3) is compared with that predicted by the standard Monte Carlo model of L99 (see Fig. 1*b*). The Monte Carlo model parameters that reproduce the range of Si isotopic ratios in presolar SiC underpredict the range of $^{18}O/^{16}O$ ratios in Group 1 and 3 oxide grains by about a factor of 8.

−2.3 (i.e., the Salpeter value adopted here), but with a spread of some ±0.3. For the model considered here, a change in IMF results in a different balance of high-mass and low-mass SNe II included in each Monte Carlo mixture. Examination of the SNe II yields (Fig. 4) indicates that the most massive SNe produce isotopically heavy Si (δ^{29}Si, δ^{30}Si > 0) and light O, whereas the least massive SNe produce isotopically light Si and heavy O. Thus, a steeper IMF slope, favoring lower mass stars, leads to lower average Si isotopic ratios for the Monte Carlo mixtures, whereas a shallower slope leads to heavier Si compositions. Using the standard model parameters discussed above (and the WW95 "B" yields), but with an IMF slope of −2.7 results in ∼20‰ lower average δ^{29}Si and δ^{30}Si values and ∼20‰ higher $^{18}O/^{16}O$ ratios for the Monte Carlo mixtures, compared to results using the Salpeter (1955) IMF. Conversely, a shallower IMF slope of −2.0 results in ∼20‰ higher Si isotopic ratios and 20‰ lower $^{18}O/^{16}O$ ratios in the mixtures. Over this range of IMF slopes, there is no appreciable change in the range of predicted isotopic ratios, nor in the degree of correlation between different isotopic pairs. Our discussions and major conclusions below are based primarily on these correlations and the relative ranges predicted for different isotopic ratios and are thus not strongly dependent on the choice of IMF. Moreover, to some extent the renormalization procedure used to scale SNe II yields depends on the chosen IMF; different renormalization factors could be chosen so that the model yields the same results for different IMFs.

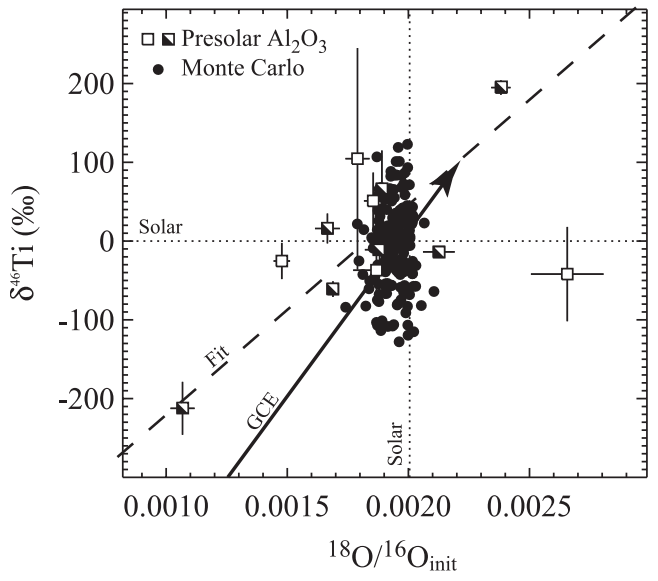

FIG. 7.—δ^{46}Ti values and inferred initial $^{18}O/^{16}O$ ratios measured in 12 Group 1 presolar Al_2O_3 grains (2 σ errors; Choi et al. 1998; Hoppe et al. 2003) are compared with predictions of the standard Monte Carlo heterogeneous GCE model (see Fig. 1*b*). Seven grains with $^{46}Ti/^{48}Ti$, $^{47}Ti/^{48}Ti$, and/or $^{49}Ti/^{48}Ti$ ratios at least 2.5 σ away from the solar values are plotted with a half-filled square symbol. Terrestrial contamination cannot be ruled out for other grains. The solid line is the homogeneous GCE model of TWW95, normalized to pass through solar; the long-dashed line is a best fit to the seven grains with Ti anomalies.

5. DISCUSSION

5.1. *Stellar Yields and Correlations*

A key result of the previous section is that, despite being able to simultaneously reproduce the range of $^{29}Si/^{28}Si$, $^{30}Si/^{28}Si$, and $^{46}Ti/^{48}Ti$ ratios observed in presolar mainstream SiC grains, the Monte Carlo model does not predict the strong linear correlation between Si and Ti isotopes exhibited by the grains. Similarly, the Monte Carlo model predicts no correlation (using the WW95 yields) or a weak anticorrelation (using the LC03 yields) between $^{18}O/^{16}O$ and $^{46}Ti/^{48}Ti$ ratios, in conflict with observations of presolar oxide grains (though the oxide data are more limited and uncertain than the SiC data.) These results can be understood by examining the bulk nucleosynthetic yields used in the Monte Carlo model. Figure 8 shows the isotopic compositions (normalized to solar values) of bulk SNe II ejecta (scaled WW95 yields) as a function of stellar mass. The high degree of correlation between $^{29}Si/^{28}Si$ and $^{30}Si/^{28}Si$ predicted by the Monte Carlo model (Fig. 1) is a direct reflection of the fact that these isotopic ratios are strongly correlated in the ejecta of SNe II of different mass. Low-mass supernovae eject Si enriched in ^{28}Si, whereas the most massive ones eject ^{28}Si-depleted Si, because of fallback of ^{28}Si onto the forming black hole. In contrast, there is little correlation between $^{29}Si/^{28}Si$ and

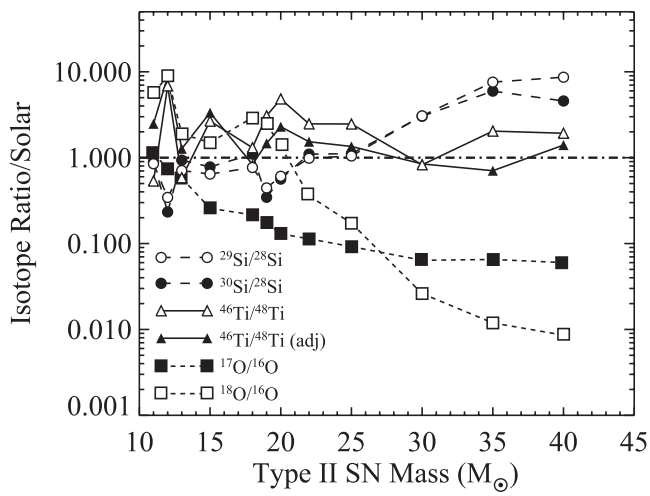

FIG. 8.—Isotopic ratios predicted for bulk SNe II ejecta as a function of progenitor mass, from the calculations of WW95 adjusted in some cases as discussed in the text. The $^{29}Si/^{28}Si$ and $^{30}Si/^{28}Si$ ratios of different mass SNe are highly correlated with each other, but not with $^{46}Ti/^{48}Ti$ or O isotopic ratios.

TABLE 1
Linear Correlation Coefficient

Isotope Ratio Pair	Grains	SN Yields (WW95)	MC Model (WW95)	SN Yields (LC03)	MC Model (LC03)
$^{29}Si/^{28}Si$–$^{30}Si/^{28}Si$	0.97	0.96	0.98	0.97	0.98
$^{29}Si/^{28}Si$–$^{46}Ti/^{48}Ti$	0.83	−0.23	0.12	0.49	0.57
		−0.32[a]	0.16[a]		
$^{17}O/^{16}O$–$^{18}O/^{16}O$	?	0.81	0.87	0.96	0.93
$^{18}O/^{16}O$–$^{46}Ti/^{48}Ti$	0.90 (0.16[b])	0.47	0.18	−0.86	−0.39
		0.81[a]	0.16[a]		
$^{29}Si/^{28}Si$–$^{18}O/^{16}O$	0.62[c]	−0.455	−0.71	−0.74	−0.64

[a] Ti-48 SNe II yields adjusted to Si and solar.
[b] Excluding two grains with most extreme isotopic anomalies (Fig. 7).
[c] Based on presolar silicate data (Mostefaoui & Hoppe 2004).

$^{46}Ti/^{48}Ti$ ratios for different SNe II masses, so mixing ejecta from different SNe into a homogeneous composition would not be expected to lead to a strong correlation between these isotopic ratios. The bulk $^{17}O/^{16}O$ and $^{18}O/^{16}O$ ratios are higher in low-mass SNe II than in higher mass ones. This in turn leads to a correlation between these isotope ratios and to an anticorrelation with Si isotope ratios in the Monte Carlo model.

The situation is summarized in Table 1, which gives the linear correlation coefficients observed for different isotope pairs in presolar grains, SNe II ejecta and predicted by the Monte Carlo model cases of Figures 1*b* and 5*a*. In several cases, the Monte Carlo model predicts slightly stronger correlations than would be expected purely from consideration of the SNe II yields. This is caused by inclusion of SNe Ia models, which for the most part are highly depleted in the heavy isotopes of Si, O and Ti, and hence introduce additional correlation. The seven presolar oxide grains with significant Ti isotopic anomalies (Fig. 7) indicate a very high correlation coefficient of 0.90 between $^{18}O/^{16}O$ and $^{46}Ti/^{48}Ti$ ratios, but this depends strongly on the two most extreme grains. Excluding these grains reduces the correlation coefficient to 0.16. Clearly, additional data are needed to clarify the situation, especially high-precision Ti isotopic measurements of grains with a wide range of $^{18}O/^{16}O$ ratios. Assuming that the oxide grains indeed define a strong ^{46}Ti–^{18}O correlation, it follows from the observed $\delta^{29}Si$–$\delta^{46}Ti$ correlation in SiC that a high positive correlation between $\delta^{29}Si$ and $\delta^{18}O$ should also hold. A correlation between these isotope ratios has in fact been seen recently for a few presolar silicate grains with O-isotopic ratios similar to the oxide grains discussed here (Mostefaoui & Hoppe 2004) and is in contrast to the high negative correlation coefficient predicted by the Monte Carlo model (last row of Table 1).

Clearly, the high degree of correlation observed between Si and Ti isotopes in the mainstream SiC grains argues strongly against inhomogeneous GCE being responsible for the bulk of the isotopic variations of the grains. As discussed by L99, the precise balance between homogeneous and inhomogeneous GCE in producing the spread in the grain data cannot be unambiguously determined from the Si isotopic data alone, since both homogeneous GCE and stochastic mixing of SNe ejecta into a homogeneous ISM result in compositions that are correlated along a line of slope $\gtrsim 1$ on the Si δ plot. However, the Si-Ti correlation observed in the grains does provide a method for estimating this balance.

The basic idea can be illustrated graphically. The distributions of SiC grains in the three-isotope plots of Figures 1 and 2 are represented in Figure 9 by ellipses whose semimajor and semiminor axes are given by the variances (2σ) in the data. Since the data are highly correlated, the principle axes of the ellipses are not parallel to the main coordinate axes. We assume that these isotope distributions reflect a superposition of smaller ellipses, corresponding to the local chemical heterogeneities arising from inhomogeneous GCE at any given time, marching up a homogeneous, average GCE trend. Figures 9*a* and 9*b* illustrate the Si ambiguity. In Figure 9*a*, the entire distribution is due to a single episode of heterogeneous GCE (*filled ellipse*), as given by the standard Monte Carlo result (Fig. 1*b*), with no contribution from homogeneous GCE. In contrast, in Figure 9*b*, the distribution is a superposition of several generations of heterogeneous SNe mixing (*filled ellipses*), each of which individually leads to only a relatively small spread in the data. Because of the highly correlated SNe II Si isotope yields, the heterogeneous GCE ellipses are of similar shape to the grain ellipse. As a result, if only Si is considered, either mix of heterogeneous and homogeneous GCE indicated by Figures 9*a* and 9*b* are plausible explanations for the data. Note that the wider spread perpendicular to the primary axis of the grains in Figure 9*b*, compared to the superposition of Monte Carlo ellipses, is easily explained by uncertainties in the grain measurements (median 2σ error in $\delta^{30}Si = 14‰$) and some spread due to variable dredge-up of Si from the He shell in the parent AGB stars. Figures 9*c* and 9*d* illustrate the same analysis for $\delta^{29}Si$ and $\delta^{46}Ti$ ratios. Because the SNe II yields for these isotopic ratios are uncorrelated, the ellipses predicted by the Monte Carlo model are much closer to circular, with principle axes parallel to the main axes, compared to the Si three-isotope result. As a result, the case illustrated by Figure 9*c* can clearly be ruled out, since the Monte Carlo (*filled*) ellipse extends far outside the spread of the data. If instead the data represent a superposition of several generations of heterogeneous GCE superimposed on a homogeneous GCE trend, the spread and correlations in both the Si (Fig. 9*b*) and Ti (Fig. 9*d*) data can be reproduced.

To be consistent with both the Si and the Ti data, the Monte Carlo model parameters can be adjusted so that the predicted $\delta^{29}Si$–$\delta^{46}Ti$ ellipse falls within the observed grain ellipse. The principle axes of the grain distribution ellipses shown in Figure 9 were determined by diagonalizing the covariance matrices for the appropriate isotope ratio pairs. For the $\delta^{29}Si$–$\delta^{46}Ti$ pair, the resulting semimajor axis has a length of 67‰ and the semiminor axis has a length of 20‰ (1σ). The semimajor axis of the standard case Monte Carlo ellipse (essentially the standard deviation of predicted $\delta^{46}Ti$ values), on the other hand, has a length of 49‰. Thus, to attain consistency, the model

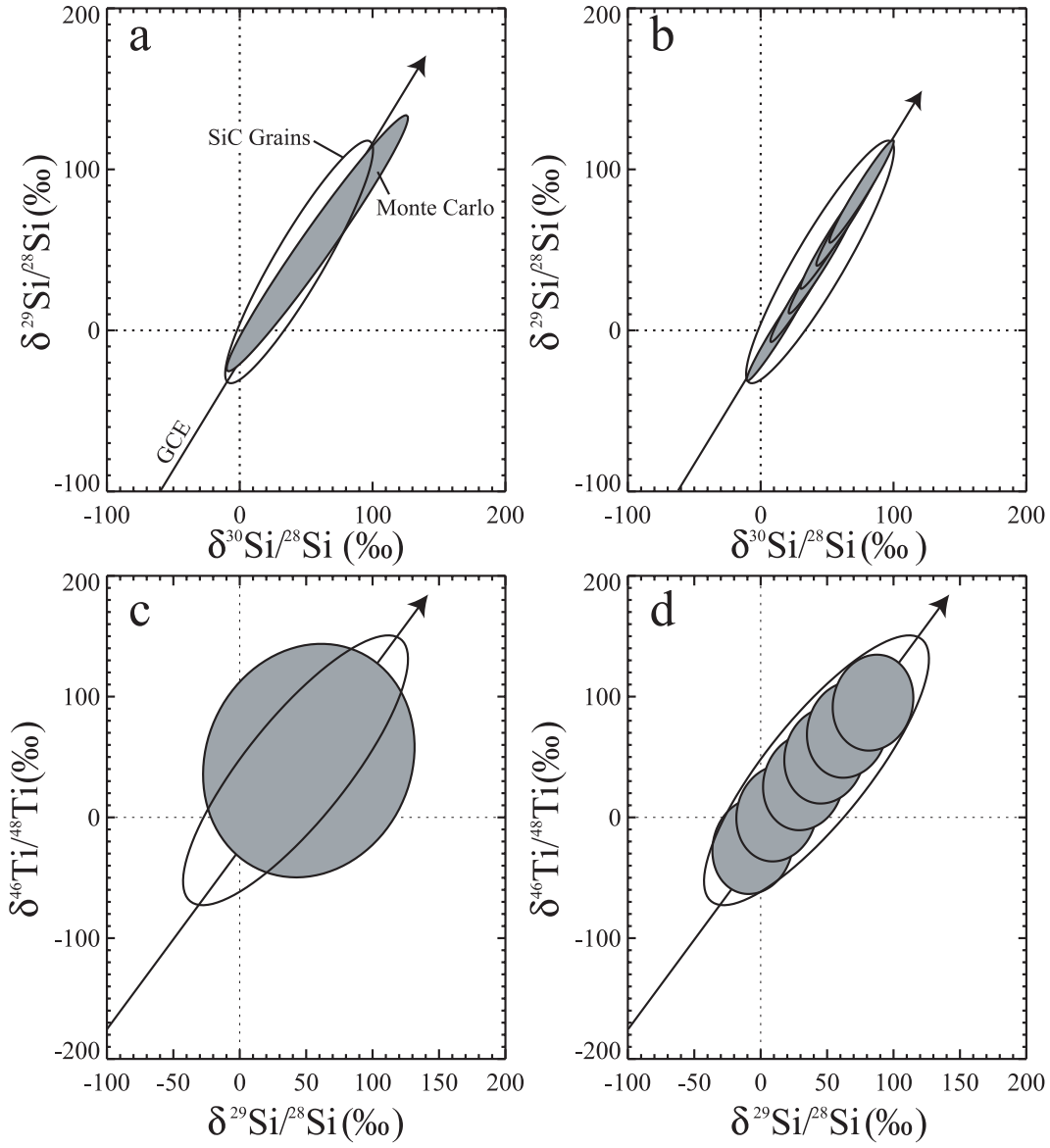

FIG. 9.—Graphical illustration of method to estimate contribution of heterogeneous GCE to presolar SiC isotopic data. Open ellipses indicate 2 σ range of SiC data on Figs. 1 and 2. Solid arrows indicate homogeneous GCE isotopic evolutionary paths. (*a*) Filled ellipse indicates range of Si isotope predictions for standard Monte Carlo model of Fig. 1*b*. In this case, the entire distribution of SiC is explained by a single generation of heterogeneous mixing of SNe ejecta into an initially homogeneous ISM. (*b*) Filled ellipses indicate several generations of heterogeneous GCE superimposed on the homogeneous GCE trend. Each generation produces a much smaller range of isotopic compositions than standard Monte Carlo model. (*c*) Same as (*a*) for δ^{46}Ti and δ^{29}Si. In this case, the Monte Carlo ellipse is clearly too wide for the grain data indicating that heterogeneous GCE cannot account for the full range of isotopic data. (*d*) Same as (*b*) for δ^{46}Ti and δ^{29}Si. This case is qualitatively compatible with both the Si and Ti isotopic data. A quantitative analysis indicates that at most 40% of the range of SiC Si isotopic ratios can be explained by the Monte Carlo model.

parameters must be adjusted to yield a spread in isotopic ratios smaller by about a factor of 2.5. Recall that the two key parameters of the model are $N_{\rm SN}$, the number of supernovae that contribute to each mix, and a, the mixing fraction from each SNe. As discussed by L99 (see their Appendix), the average composition of the Monte Carlo mixtures is fixed by the product $a \times N_{\rm SN}$. L99 suggested that the predicted spread around the average is determined mainly by $N_{\rm SN}$ (in fact proportional to $1/N_{\rm SN}^{1/2}$). However, we find that for $N_{\rm SN} \lesssim 1000$, a has a bigger effect on the isotopic spread, with the standard deviation of isotope ratios varying roughly in proportion to a. In any case, there are a range of parameters that can result in the smaller isotopic spread required by the Si-Ti correlation. Figures 1*d* and 2*d* show the results for the case $N_{\rm SN} = 70$ and $a = 5.5 \times 10^{-6}$. With these parameters, the standard deviation of the predicted δ^{46}Ti values is 20‰, just consistent with the spread in the grain data. If $N_{\rm SN}$ is raised to 400, then a value of $a \approx 3 \times 10^{-6}$ gives very similar results. Shown in Figures 5*c* and 5*d* are the results of the same exercise applied to the Monte Carlo model using the LC03 SNe II yields. In this case, parameter values of $a = 1.3 \times 10^{-5}$ and $N_{\rm SN} = 70$ provide an isotopic spread consistent with the Si-Ti grain correlation.

Thus, taking into account the correlation between Si and Ti isotopes in presolar SiC grains, inhomogeneous GCE can account for about 40% of the observed spread in the SiC isotopic data. This result is obtained using either the SNe II yields of WW95 or those of LC03. However, this is in fact an upper limit, for several resons. First, this result is essentially based on the maximal variation in δ^{46}Ti values at a given δ^{29}Si value in the grains. Some of this variation ($\sim$20‰ 1 σ, based on the width of the grain ellipse in Figs. 9*c* and 9*d*) is certainly due to analytical uncertainties in the grain data. Reported errors on the SiC δ^{46}Ti

values have a mean value of ~17‰. Second, some of the spread in δ^{46}Ti must be due to varying amounts of He-shell material dredged up in the parent AGB stars of the grains (Fig. 2*a*). There are major uncertainties in the expected He-shell Ti isotope composition, but the range expected for low-mass C-rich AGB stars is at least 20‰ (L99). Third, ^{29}Si/^{28}Si is also strongly correlated with ^{47}Ti/^{48}Ti, ^{49}Ti/^{48}Ti, and, to a lesser extent, ^{50}Ti/^{48}Ti ratios in mainstream SiC grains (Hoppe et al. 1994; Alexander & Nittler 1999). However, as discussed earlier, current SNe II models greatly underproduce ^{47}Ti, ^{49}Ti, and ^{50}Ti, and these isotopes are now believed to be produced in nature primarily in rare types of SNe Ia (WW95; TWW95). Since the heavy Si isotopes are produced in SNe II, any heterogeneous GCE model would thus be expected to result in even less correlation between Si isotopes and these other Ti isotopes and in fact might even lead to anticorrelations. Thus, these considerations indicate that, at most 40%, and probably less, of the Si and Ti isotopic spread in presolar SiC grains is due to heterogeneous mixing of SNe ejecta in the ISM. Some broader implications of this result for GCE are discussed below in § 5.3.

One might reasonably ask at this point whether the lack of correlation between the Si and Ti SNe II rare isotope yields is merely due to uncertainties in the nucleosynthetic calculations. This appears to be quite unlikely since the different isotopes are produced by different processes in different mass zones within SNe. For example, ^{29}Si and ^{30}Si are produced by the same processes, mainly shell O-burning (TC96), and hence their yields are correlated. In contrast, ^{46}Ti is made by explosive O burning, and its yield is correlated with that of ^{28}Si, which is also made by this process in the same inner zones of SNe II. Although SNe II models underproduce ^{48}Ti, it is difficult to conceive of a situation where its yields would conspire to introduce a strong correlation between ^{46}Ti/^{48}Ti and ^{29}Si/^{28}Si as observed in the grains. Moreover, as discussed in the previous paragraph, a significant fraction of ^{47}Ti, ^{49}Ti, and ^{50}Ti are probably made in rare types of SNe Ia, and thus the correlations between these and ^{29}Si/^{28}Si in SiC could not be explained by any adjustment of SNe II yields. Finally, the basic agreement between the models using the WW95 yields and those using the LC03 yields indicates that the conclusion that heterogeneous GCE does not produce a strong correlation between the Si and Ti isotopic ratios is quite robust.

5.2. *Comparison of Presolar* SiC *and Presolar Oxide Grains*

Mainstream presolar SiC grains and Group 1 and 3 presolar oxide grains both originated in the winds from low-mass stars during their red giant and AGB phases (see § 2). It would thus be expected that two grain populations formed in similar populations of stars. Identical populations would not be expected, however, since oxide grains can form during the RGB and O-rich AGB phases of stellar evolution, but SiC only during the C-rich AGB phase. For example, whereas all stars start out O-rich, only a limited mass range of stars probably ever become C-rich and thus SiC producers (Straniero et al. 1997). Thus, although it possible that the stars that made the SiC grains also made some of the oxide grains earlier in their evolution, there could be many presolar oxide grains from stars that never became C rich. Based on homogeneous GCE models, previous studies have concluded that the parent stars of presolar oxide grains had a wider range of metallicities than did the SiC progenitors (e.g., Fig. 3 of Alexander & Nittler 1999). This conclusion depends on the observation that the relative range of ^{18}O/^{16}O ratios in presolar oxides (Fig. 6) is much wider than the range of Si isotopic ratios in mainstream SiC grains (Fig. 1). One motivation for the present work was to determine whether inhomogeneous GCE could help explain the different isotopic ranges of the grains, rather than invoking different metallicity distributions for the parent stars. Unfortunately, the results described in the previous sections make clear that heterogeneous mixing of SNe ejecta into an initially homogeneous ISM cannot simultaneously explain the range of ^{18}O/^{16}O in the oxide grains and ^{29}Si/^{28}Si in the presolar SiC grains. The L99 Monte Carlo model, when tuned to explain the range of Si isotopic ratios in the SiC grains, predicts a range in ^{18}O/^{16}O about 8 times smaller than is indicated by the presolar oxide grains. When the results of the previous section are considered, it is obvious that only a negligible fraction of the O-isotopic range in presolar oxide grains can be explained by inhomogeneous GCE.

Inferring metallicity distributions for presolar grain parent stars requires knowledge of how isotopic ratios evolve with metallicity during GCE. Previous estimates (Nittler 1997; Alexander & Nittler 1999) have been based on the homogeneous GCE calculations of TWW95 and TC96. However, from both theoretical and observational standpoints, the GCE of O isotopes is poorly understood (e.g., Prantzos et al. 1996). For example, observations of molecular clouds indicate that both ^{17}O and ^{18}O act as secondary isotopes and their abundance should increase with metallicity, relative to ^{16}O. A major problem, however, is that the Sun has an ^{18}O/^{17}O ratio of 5.2, 1.5 times higher than the value of ≈3.5 measured in molecular clouds throughout the Galaxy (Wilson & Rood 1994). Nonetheless, Nittler et al. (1997) showed that the distribution of O isotopic ratios in presolar oxide grains is well explained by assuming a simple linear relationship between ^{18}O/^{16}O and metallicity in the Galaxy. Moreover, even if the *absolute* relationship between isotopic ratios and metallicity is unknown, we can use the presolar grain data themselves to infer *relative* evolutionary rates of the different isotope systems. In particular, the fact that Ti isotopes can be measured in both SiC and oxide minerals provides a way to intercompare the Si and O isotope GCE. Fitting a line to the δ^{46}Ti–δ^{29}Si SiC data of Figure 2*a* gives a slope of 1.09, i.e., a 10% increase in ^{29}Si/^{28}Si corresponds to a similar increase in ^{46}Ti/^{48}Ti. A similar fit to the Ti-O data of the presolar oxide grains (e.g., Fig. 7, *dashed line*) gives a slope of 0.5, when ^{18}O/^{16}O is expressed as δ^{18}O. Thus, the Ti-Si and Ti-O correlations imply that ^{18}O/^{16}O evolves twice as fast as ^{29}Si/^{28}Si. The O and Si isotope data recently reported for a few presolar silicate grains (Mostefaoui & Hoppe 2004) appear quite consistent with this, although the errors on the isotopic ratios are relatively large. The standard deviation of the oxide grain ^{18}O/^{16}O distribution (24%) is in fact 6.3 times higher than the width of the SiC Si distribution (3.8%). Thus, even without an absolute isotope-metallicity scale, we can conclude that the oxide grains formed in stars with a ~3 times wider range in metallicity than the parent stars of the SiC grains.

The parent stars of presolar oxide grains might be expected to have a wider metallicity range than the SiC parents, if they also have a wider range of masses. The lower mass limit of C-rich AGB stars is ~1.5 $M_\odot$ (Straniero et al. 1997), but many of the oxide grains, especially the Group 3 grains, are estimated to have come from lower mass stars (Nittler 1997), based on comparison of their ^{17}O/^{16}O ratios with the dredge-up models of Boothroyd & Sackmann (1999). Since lower mass stars evolve on longer timescales than do higher mass stars, the lower mass parents would necessarily have formed earlier in Galactic history. Assuming an age-metallicity relationship for the Galaxy then implies lower metallicity on average for the parent stars of these grains than the parent stars of the SiC grains (see also Nittler

et al. 1997). However, this explanation is not sufficient to explain the wider metallicity range of the oxide grain parents. Calculations of the effects of the first dredge-up on O isotopes indicate that $^{17}O/^{16}O$ ratios greater than 2×10^{-3} are only obtained in red giants that are more massive than 2 $M_{\odot}$ (e.g., Boothroyd & Sackmann 1999). The Group 1 presolar oxide grains with $^{17}O/^{16}O$ in this range show almost as wide a range of $^{18}O/^{16}O$ as the total grain distribution (Fig. 3), implying almost as wide a metallicity range. Thus, even the parent stars of oxide grains that had similar masses to the SiC grain parents ($\sim$2 $M_{\odot}$, L99) apparently had a wider range of metallicity.

The preceding discussion is based on the assumption that the first dredge-up is the only stellar process that affected the $^{18}O/^{16}O$ ratios in the parent stars of the Group 1 and 3 oxide grains. However, low-mass red giants are observed to undergo an additional mixing process, often called cool bottom processing (CBP), not predicted by standard stellar evolutionary models. CBP results in partial H-burning of the stellar envelope material itself, resulting in low $^{12}C/^{13}C$ ratios observed in low-mass red giants (Charbonnel 1994; Boothroyd & Sackmann 1999). Moreover, CBP during the AGB phase has been shown to be a plausible explanation for the anomalously low $^{18}O/^{16}O$ ratios and high inferred $^{26}Al/^{27}Al$ ratios measured in Group 2 presolar oxide grains (Fig. 3; Wasserburg et al. 1995; Nollett et al. 2003). It is possible that the parent stars of most Group 1 and 3 oxide grains underwent a limited amount of CBP, leading to a wider range of $^{18}O/^{16}O$ ratios than was present in the initial compositions of the stars. The Group 1 grains with $^{17}O/^{16}O \gtrsim 2 \times 10^{-3}$ appear to form a distinct trend from Group 2 grains, for which CBP has clearly played a significant role. However, a minor effect of CBP on these grains cannot be ruled out.

Perhaps the best hope for resolving the relationship between the parent stars of presolar oxide grains and presolar SiC grains are presolar silicate minerals, since these contain abundant Si and O. Presolar silicates have recently been discovered in interplanetary dust particles (Messenger et al. 2003) and meteorites (Nguyen & Zinner 2004; Nagashima et al. 2004; Mostefaoui & Hoppe 2004). Only limited Si isotopic data have been reported for these grains so far, but such data could potentially provide a direct comparison of the evolutionary rates of Si and O isotopes during GCE.

5.3. *Implications for Galactic Evolution*

The previous discussions have focused specifically on the implications of the Monte Carlo results for interpreting the presolar grain data themselves. However, the grains formed around a number of low-mass stars that happened to end their lives and inject dust into the ISM close in time (probably within 10^7–10^8 yr) and space to the formation of the solar system. They thus represent a complementary sample to modern observational studies of abundances in low-mass stars in the solar neighborhood (e.g., Edvardsson et al. 1993; Reddy et al. 2003) and chemical abundance variations inferred for their parent stars might be used to draw broader conclusions about Galactic evolution. However, because we cannot identify a specific grain with a specific (now dead for billions of years) star, we must first ask whether the grains are a representative sample of the stars present near the protosolar cloud. Based on the range of isotopic compositions measured in the grains, at least a few tens of individual C stars must have contributed SiC grains to the solar system (Alexander 1993, 1997). Moreover, the distribution of $^{12}C/^{13}C$ ratios measured in the SiC grains matches that measured spectroscopically in present-day C stars astonishingly well (Smith & Lambert 1990; Hoppe et al. 1994). Lodders & Fegley (1998) considered in detail the properties of a large number of observed C stars and presolar SiC grains and concluded that the SiC grains formed in a population of C stars roughly similar to the present-day C star distribution, though possibly with lower metallicities. All of these observations suggest that the SiC originated in a reasonably representative sample of C stars in a restricted part of the Galaxy some 4.5 billion years ago.

TABLE 2

Spread in Elemental Abundances Predicted by "Maximal" Monte Carlo Model

Ratio	Standard Deviation		
	Monte Carlo[a]	Monte Carlo[b]	Astronomical Limits[c]
[Mg/Fe].....	0.0047	0.0054	0.04
[Si/Fe].....	0.0038	0.0046	0.05
[Al/Fe].....	0.0070	0.0080	0.05
[Ca/Fe]	0.0033	0.0035	0.04
[Ti/Fe].....	0.015	0.016	0.04

[a] WW95 SNe II Fe yields.
[b] WW95 SNe II Fe yields times 0.5.
[c] Reddy et al. (2003).

The Monte Carlo heterogeneous GCE model discussed here of course leads to variations in elemental abundance ratios as well as isotopic variations. L99 showed that Monte Carlo model parameters that reproduced the mainstream SiC Si isotopic distribution led to variations in major element abundances (e.g., Mg/Fe, Ca/Fe) comparable to the scatter observed in solar neighborhood stars by Edvardsson et al. (1993). However, the relative elemental variations in the Edvardsson et al. (1993) data set are dominated by observational errors, so it is possible that the intrinsic variations in present-day stars are actually much smaller than those predicted by the Monte Carlo model. We showed above that the observed correlation between Si and Ti isotopes in SiC grains provides an upper limit on the amount of chemical heterogeneity allowed due to inhomogeneous mixing of SNe ejecta in the ISM. Taking the "maximal" Monte Carlo model, which is just consistent with the distribution of Si and Ti isotopic ratios in SiC grains (Figs. 1*d* and 2*d*), we have calculated the expected corresponding spread in a few major element abundance ratios commonly measured spectroscopically in stars. These are upper limits on the abundance spreads expected for a single stellar generation, or equivalently stars of closely similar metallicity. Table 2 shows the results, given as the standard deviation of the ratios expressed in the common bracketed logarithmic notation. We have performed the calculations with both the original WW95 Fe yields and with these yields halved, according to TWW95. The standard deviations of [Fe/H] for these two cases are 0.030 and 0.022, respectively, and are much smaller than the $\sim$0.2 dispersion observed by Edvardsson et al. (1993) for stars of the same age. Also shown are the dispersions in the element ratios ("cosmic scatter") reported by Reddy et al. (2003). The latter are upper limits because the observed scatter in abundances is comparable to the estimated observational errors. Figure 10 also illustrates the comparison between our predicted spreads in element ratios and the astronomical uncertainties. For each of the plotted element ratios, the entire range of predictions lies within ellipses corresponding to 1 σ uncertainty in the spectroscopic results (Reddy et al. 2003).

As discussed in § 1, Reddy et al. (2003) concluded that the ejecta from diverse nucleosynthesis sources is well mixed in the ISM. Additional evidence that the ISM is well mixed comes

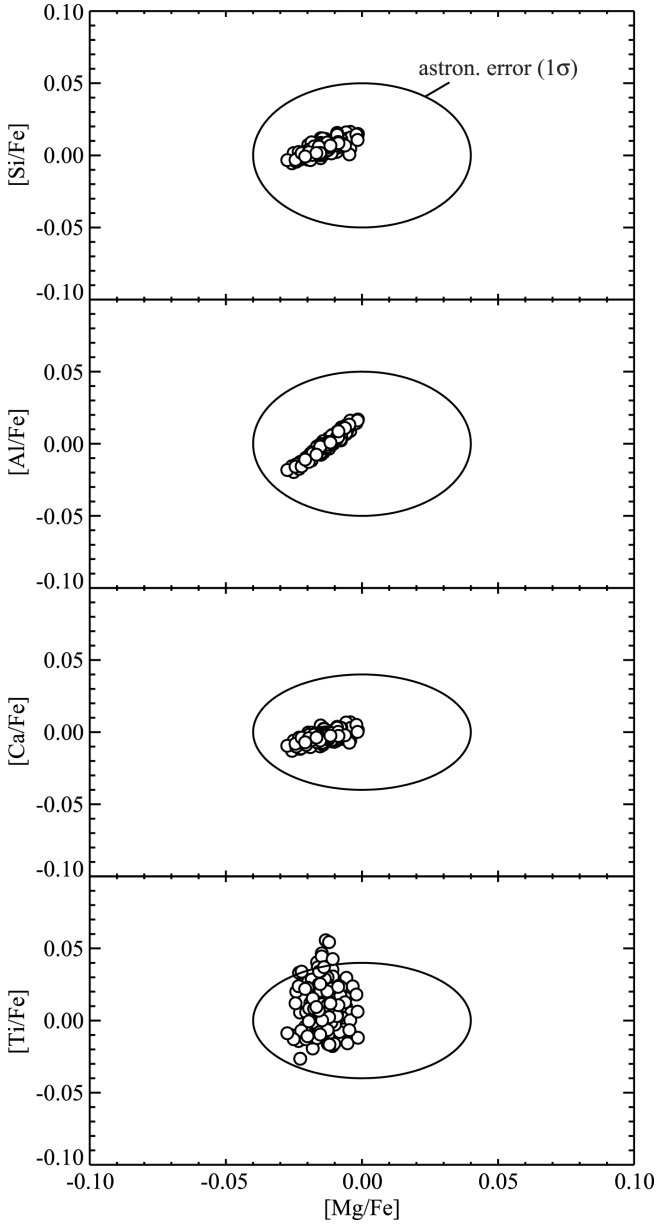

FIG. 10.—Predicted ranges of element ratios ($[el/Fe] = \log(el/Fe) - \log(El/Fe)_{\odot}$) predicted by "maximal" Monte Carlo model allowed by Si-Ti correlation in SiC grains (Figs. 1*d* and 2*d*) compared with astronomical uncertainties. Only results for the model using standard WW95 Fe yields (Table 2) are shown. The predicted ranges are all within ± 1 σ error ellipses of astronomical measurements (Reddy et al. 2003), indicating that the presolar grains provide much more stringent limits on "cosmic scatter" than can be observationally determined.

from gas-phase C, N, O, and Kr abundance measurements along various lines of sight in the Galaxy (e.g., Cartledge et al. 2003 and references therein). These observations show no significant variation outside uncertainties (of comparable scale to the stellar data) for lines of sight within the local spiral arm. The presolar grain data discussed here, especially the strong correlation between Si and Ti isotopes, provide much more stringent limits on the cosmic scatter than can be derived from the astronomical results. The upper limits we place on the deviations of [el/Fe] ratios in Table 2 are in several cases an order of magnitude smaller than the limits derived by Reddy et al. (2003). Note that a dispersion of 0.005 dex (as derived for [Mg/Fe]) corresponds to a linear variation of $\sim$1%. Our results thus imply that the ejecta from discrete SNe explosions are remarkably locally well-mixed, to a percent level, in the ISM. Conversely, if low-mass stars in the solar neighborhood some 4.5 billion years ago had a larger spread in element/Fe ratios than this, then the SiC grains should not show the strong correlation between Si and Ti isotopic ratios that is observed. It remains to be seen whether the highly efficient mixing of the ISM implied by the data can be understood in the context of Galactic mixing processes. For example, recent work by De Avillez & Mac Low (2002) finds that initial 10–50 pc scale heterogeneities in the Galaxy are homogenized to the several percent level on a timescale of tens of Myr with faster homogenization occurring for higher supernova rates.

Strictly speaking, our conclusion that the ISM is very well mixed is limited to the time period over which the presolar grains were formed and injected into the ISM, roughly 4.5–5.5 Gyr ago. The observational evidence cited above suggests that the high degree of mixing in the ISM has continued since then, but the data do not require the same level of mixing during earlier epochs of Galactic evolution. In fact, heterogeneous GCE due to inhomogeneous mixing of SNe ejecta in the ISM was probably much more important in the early Galaxy (Argast et al. 2000; Oey 2000, 2003).

Clayton (2003) recently offered a completely different interpretation for the mainstream SiC isotopic data discussed here, and indeed for the presolar chemical and dynamical history of the solar neighborhood. He postulates that the linear arrays of Si and Ti isotopic ratios on three-isotope plots do not represent a marching up of isotopic ratios due to standard homogeneous GCE theory, but rather they are mixing lines due to a merger of a dwarf galaxy with the Milky Way disk. Isotopic compositions of the grains reflect both mixing of gas from the two galaxies and subsequent enrichment by SNe formed in a burst of star formation triggered by the merger event itself. Although this model is speculative, it can apparently explain several features of the SiC data, especially the correlations between Si and Ti isotopic ratios, the steep slope of the Si isotope data on a δ plot (Fig. 1) and the isotopically heavy Si in the grains relative to the Sun. Much more detailed investigation of this model is needed to determine whether it makes any predictions that could definitively test it (e.g., diagnostic isotopic ratios, possible observational signatures) against the standard GCE interpretation of the grain data. In the context of the present paper, we note that our Monte Carlo results neither support nor contradict the merger idea. However, our basic conclusion that local heterogeneities due to incomplete mixing of SNe ejecta in the ISM are relatively small is equally valid whether the SiC isotope correlation lines are due to homogeneous GCE or to mixing of gas from merging galaxies.

6. SUMMARY AND CONCLUDING REMARKS

In this paper, we have applied the Monte Carlo heterogeneous GCE model of L99 to the combined isotopic systems of Si, Ti, and O. Our basic conclusions can be summarized as follows.

1. Although model parameters can be chosen so that the entire range of Si isotopic ratios in mainstream presolar SiC grains is reproduced purely by locally heterogeneous mixing of SNe ejecta in the ISM, this model does not reproduce the strong correlation between $^{29}Si/^{28}Si$ and $^{46}Ti/^{48}Ti$ ratios observed in the grains. This result reflects the fact that the Si and Ti isotopes are made by different processes and the yields from SNe II of different masses are hence uncorrelated. No model that relies on stochastic mixing of ejecta from different SNe would reproduce the isotopic correlations observed in the grains. The

degree of correlation between $^{29}Si/^{28}Si$ and $^{46}Ti/^{48}Ti$ ratios in the SiC grains implies an upper limit of 40% for the contribution of the heterogeneous GCE model to the total range of SiC compositions.

2. The Monte Carlo model cannot simultaneously explain the range of Si and Ti isotopes in presolar SiC grains and the range of $^{18}O/^{16}O$ ratios in presolar oxide grains, despite the fact that the grain types come from roughly similar types of stars. Ti isotopic data for both SiC grains and a few presolar Al_2O_3 grains provide a relative metallicity scale for the two grain types and indicate that the oxide grains formed in stars with about 3 times wider range in metallicity than the stars that produced SiC grains. One possible explanation for this discrepancy is that the oxide grain parent stars underwent limited cool bottom processing leading to a larger range of $^{18}O/^{16}O$ ratios than is expected solely from dredge-up processes in red giants.

3. If, as is likely, the mainstream presolar SiC grains originated in a representative sample of low-mass stars in the region of solar system formation, then the Si–Ti isotope correlation also limits the amount of scatter in element/iron ratios in stars of a given metallicity. Monte Carlo model parameters just allowed by the Si–Ti correlation predict total scatter in elemental ratios like Mg/Fe and Si/Fe on the order of 1%. This is an order of magnitude smaller than can be resolved with present astronomical measurements and indicates that ejecta from diverse nucleosynthetic sources are remarkably locally well-mixed in the ISM.

It is now clear from observations of stars (Edvardsson et al. 1993, Reddy et al. 2003), interstellar gas phase abundances (Cartledge et al. 2003), and presolar grains in meteorites (this work) that the ISM is chemically well mixed. Disk stars of a given overall metallicity have a relatively narrow range of chemical and isotopic compositions, in most cases probably determined by traditional GCE processes. The data indicate that the large scatter in metallicity for stars of a given age cannot be explained by heterogeneous mixing of stellar ejecta in different local regions. Rather, this scatter probably requires an origin in processes that do not affect relative elemental and isotopic abundances, including radial migration of stellar orbits and/or heterogeneous infall and mixing of low-metallicity material onto the disk.

The author is grateful to Maria Lugaro for clarifying many details of her Monte Carlo model and for providing some supernova yields and Conel Alexander for a careful reading of the manuscript. The paper was improved by comments from two anonymous referees. This work was supported by NASA grant NAG5-12917.

REFERENCES

Alexander, C. M. O'D. 1993, Geochim. Cosmochim. Acta, 57, 2869
———. 1997, in AIP Conf. Proc. 402, Astrophysical Implications of the Laboratory Study of Presolar Materials, ed. T. J. Bernatowicz & E. Zinner (New York: AIP), 567
Alexander, C. M. O'D., & Nittler, L. R. 1999, ApJ, 519, 222
Amari, S., Nittler, L. R., Zinner, E., Gallino, R., Lugaro, M., & Lewis, R. S. 2001, ApJ, 546, 248
Anders, E., & Zinner, E. 1993, Meteoritics 28, 490
Argast, D., Samland, M., Gerhard, O. E., & Thielemann, F.-K. 2000, A&A, 356, 873
Blackmon, J. C., Champagne, A. E., Hofstee, M. A., Smith, M. S., Downing, R. G., & Lamaze, G. P. 1995, Phys. Rev. Lett., 74, 2642
Boothroyd, A. I., & Sackmann, I.-J. 1999, ApJ, 510, 232
Boothroyd, A. I., Sackmann, I.-J., & Wasserburg, G. J. 1994, ApJ, 430, L77
Cappellaro, E., Evans, R., & Turatto, M. 1999, A&A, 351, 459
Cartledge, S. I. B., Meyer, D. M., & Lauroesch, J. T. 2003, ApJ, 597, 408
Chabrier, G. 2003, PASP, 115, 763
Charbonnel, C. 1994, A&A, 282, 811
Choi, B.-G., Huss, G. R., Wasserburg, G. J., & Gallino, R. 1998, Science, 282, 1284
Clayton, D. D. 1988, ApJ, 334, 191
———. 1997, ApJ, 484, L67
———. 2003, ApJ, 598, 313
Clayton, D. D., & Nittler, L. R. 2004, ARA&A, 42, 39
Clayton, D. D., & Timmes, F. X. 1997, ApJ, 483, 220
Copi, C. J. 1997, ApJ, 487, 704
de Avillez, M. A., & Mac Low, M. 2002, ApJ, 581, 1047
Edvardsson, B., Anderson, J., Gustaffson, B., Lambert, D. L., Nissen, P. E., & Tomkin, J. 1993, A&A, 275, 101
François, P., & Matteucci, F. 1993, A&A, 280, 136
Gallino, R., Raiteri, C. M., Busso, M., & Matteucci, F. 1994, ApJ, 430, 858
Hoppe, P., Amari, S., Zinner, E., Ireland, T., & Lewis, R. S. 1994, ApJ, 430, 870
Hoppe, P., Nittler, L. R., Mostefaoui, S., Alexander, C. M. O'D., & Marhas, K. K. 2003, 34th Annu. Lunar Planet. Sci. Conf., abstract 1570
Hoppe, P., & Ott, U. 1997, in AIP Conf. Proc. 402, Astrophysical Implications of the Laboratory Study of Presolar Materials, ed. T. J. Bernatowicz & E. Zinner (New York: AIP), 27
Huss, G. R., Hutcheon, I. D., & Wasserburg, G. J. 1997, Geochim. Cosmochim. Acta, 61, 5117
Ireland, T. R., Zinner, E. K., & Amari, S. 1991, ApJ, 376, L53
José, J., & Hernanz, M. 1998, ApJ, 494, 680
Kaeppeler, F., et al. 1994, ApJ, 437, 396
Kroupa, P. 2002, Science, 295, 82
Limongi, M., & Chieffi, A. 2003, ApJ, 592, 404 (LC03)
Lodders, K., & Fegley, B. 1998, Meteoritics Planet. Sci., 33, 871
Lugaro, M., Gallino, R., Amari, S., Zinner, E., & Nittler, L. R. 2003, Nucl. Phys. A, 718, 419C
Lugaro, M., Gallino, R., Zinner, E., & Amari, S. 2001, Meteoritics Planet. Sci., 36, A118
Lugaro, M., Zinner, E., Gallino, R., & Amari, S. 1999, ApJ, 527, 369 (L99)
Malinie, G., Hartmann, D. H., Clayton, D. D., & Mathews, G. J. 1993, ApJ, 413, 633
McWilliam, A. 1997, ARA&A, 35, 503
Messenger, S., Keller, L. P., Stadermann, F. J., Walker, R. M., & Zinner, E. 2003, Science, 300, 105
Mostefaoui, S., & Hoppe, P. 2004, ApJ, 613, L149
Nagashima, K., Krot, A., & Yurimoto, H. 2004, Nature, 428, 921
Nguyen, A., & Zinner, E. 2004, Science, 303, 1496
Nittler, L. R. 1997, in AIP Conf. Proc. 402, Astrophysical Implications of the Laboratory Study of Presolar Materials, ed. T. J. Bernatowicz & E. Zinner (New York: AIP), 59
———. 2002, 33rd Annu. Lunar Planet. Sci. Conf., Abstract 1650
———. 2003, Earth Planet. Sci. Lett., 209, 259
Nittler, L. R., & Alexander, C. M. O'D. 1999, ApJ, 526, 249
———. 2003, Geochim. Cosmochim. Acta, 67, 4961
Nittler, L. R., Alexander, C. M. O'D., Gao, X., Walker, R. M., & Zinner, E. 1997, ApJ, 483, 475
Nollett, K. M., Busso, M., & Wasserburg, G. J. 2003, ApJ, 582, 1036
Nomoto, K., Iwamoto, K., Nakasato, N., Thielemann, F.-K., Brachwitz, F., Tsujimoto, T., Kubo, Y., & Kishimoto, N. 1997, Nucl. Phys. A. 621, 467
Oey, M. S. 2000, ApJ, 542, L25
———. 2003, in IAU Symp. 212, A Massive Star Odyssey: From Main Sequence to Supernova, ed. K. van der Hucht, A. Herrero, & E. César (San Francisco: ASP), 620
Pilyugin, L. S., & Edmunds, M. G. 1996, A&A, 313, 792
Prantzos, N., Aubert, O., & Audouze, J. 1996, A&A, 309, 760
Rauscher, T., Heger, A., Hoffman, R. D., & Woosley, S. E. 2002, ApJ, 576, 323
Reddy, B. E., Tomkin, J., Lambert, D. L., & Allende Prieto, C. 2003, MNRAS, 340, 304
Rocha-Pinto, H. J., Maciel, W. J., Scalo, J., & Flynn, C. 2000, A&A, 358, 850
Salpeter, E. E. 1955, ApJ, 121, 161
Sellwood, J. A., & Binney, J. J. 2002, MNRAS, 336, 785
Smith, V. V., & Lambert, D. L. 1990, ApJS, 72, 387
Straniero, O., Chieffi, A., Limongi, M., Busso, M., Gallino, R., & Arlandini, C. 1997, ApJ, 478, 332
Thielemann, F. K., Nomoto, K., & Yokoi, K. 1986, A&A, 158, 17

Timmes, F. X., & Clayton, D. D. 1996, ApJ, 472, 723 (TC96)
Timmes, F. X., Woosley, S. E., & Weaver, T. A. 1995, ApJS, 98, 617 (TWW95)
van den Hoek, L., & de Jong, T. 1997, A&A, 318, 231
Wasserburg, G. J., Boothroyd, A. I., & Sackmann, I.-J. 1995, ApJ, 447, L37
Wielen, R., Fuchs, B., & Dettbarn, C. 1996, A&A, 314, 438
Wilson, T. L., & Rood, R. T. 1994, ARA&A, 32, 191
Woosley, S. E., & Weaver, T. A. 1994, ApJ, 423, 371
———. 1995, ApJS, 101, 181 (WW95)
Zinner, E. 1998, Annu. Rev. Earth Planet. Sci., 26, 147
Zinner, E., Amari, S., Guinness, R., Nguyen, A., Stadermann, F., Walker, R. M., & Lewis, R. S. 2003, Geochim. Cosmochim. Acta, 67, 5083